

Lawrence Berkeley National Laboratory

LBL Publications

Title

On the propagation of a disturbance in a heterogeneous, deformable, porous medium saturated with two fluid phases

Permalink

<https://escholarship.org/uc/item/2hk8s0kr>

Journal

Geophysics, 77(3)

ISSN

0016-8033

Authors

Vasco, DW
Minkoff, SE

Publication Date

2012

DOI

10.1190/geo2011-0131.1

Peer reviewed

On the propagation of a disturbance in a heterogeneous, deformable, porous medium saturated with two fluid phases

D. W. Vasco¹ and Susan E. Minkoff²

ABSTRACT

The coupled modeling of the flow of two immiscible fluid phases in a heterogeneous, elastic, porous material is formulated in a manner analogous to that for a single fluid phase. An asymptotic technique, valid when the heterogeneity is smoothly varying, is used to derive equations for the phase velocities of the various modes of propagation. A cubic equation is associated with the phase velocities of the longitudinal modes. The coefficients of the cubic equation are expressed in terms of sums of the determinants of 3×3 matrices whose elements are the parameters found in the governing equations. In addition to the three longitudinal modes, there is a transverse mode of propagation, a generalization of the elastic shear wave. Estimates of the phase velocities for a homogeneous medium, based upon the formulas in this paper, agree with previous studies. Furthermore, predictions of longitudinal and transverse phase velocities, made for the Massillon sandstone containing varying amounts of air and water, are compatible with laboratory observations.

INTRODUCTION

Multiphase flow is an important physical process that underlies many critical activities such as waste disposal, geothermal production, oil and gas production, agriculture, and groundwater management. Geophysical imaging methods are used increasingly to monitor the flow of liquids and gases in the subsurface (Calvert, 2005; Rubin and Hubbard, 2006). Therefore, it is important to have accurate and efficient techniques for modeling wave propagation in heterogeneous porous media saturated by one or more fluid phases. It is particularly helpful to have methods that provide insight into

the various physical factors controlling the propagation of a wave in a poroelastic medium.

There are several ways to approach the coupled modeling of deformation and multiphase fluid flow in a heterogeneous porous medium, each with its own advantages and limitations. A numerical method is the most general, and there are several studies based upon numerical techniques (Noorishad et al., 1992; Rutqvist et al., 2002; Minkoff et al., 2003, 2004; Dean et al., 2006). Numerical methods can require significant computer resources — CPU time and computer memory. Also, numerical methods have difficulty modeling the wide range of behaviors in the coupled multiphase problem, which can include hyperbolic elastic wave propagation as well as fluid diffusion, involving a broad range of time scales: from milliseconds to hours or even days. Numerical methods tailored to seismic frequencies can improve the computational efficiency (Masson et al., 2006) but still face challenges in treating multiple fluid phases and 3D problems. Finally, numerical methods do not provide explicit expressions for observed quantities such as the arrival time of a propagating disturbance or its amplitude. Analytic methods can be efficient and can provide explicit expressions for observed quantities. However, analytic methods are typically limited to relatively simple situations, such as a homogeneous half-space and a single fluid phase (Levy, 1979; Simon et al., 1984; Gajo and Mongiovi, 1995). As the medium is generalized — for example, by including layering — analytic methods become increasingly complicated and require significantly more computation time, facing the same limitations as numerical techniques (Wang and Kumpel, 2003). Thus, analytic methods may not provide the generality required for solving commonly encountered inverse problems. For example, in many inverse problems, one is interested in determining smoothly varying heterogeneous properties in a 3D setting.

In this paper, we formulate and validate governing equations for deformation in a porous medium containing two fluid phases and present an asymptotic, semianalytic technique for their solution. The equations, presented below, are generalizations of those for a medium containing a single fluid, given by Pride et al. (1992)

Manuscript received by the Editor 2 April 2011; revised manuscript received 12 December 2011; published online 9 April 2012.

¹Lawrence Berkeley Laboratory, Earth Sciences Division, Berkeley, California, USA. E-mail: dwvasco@lbl.gov.

²University of Maryland Baltimore County, Department of Mathematics and Statistics, Baltimore, Maryland, USA. E-mail: sminkoff@umbc.edu.

© 2012 Society of Exploration Geophysicists. All rights reserved.

and Pride (2005). The governing equations share many characteristics with earlier work by Tuncay and Corapcioglu (1996, 1997) and Lo et al. (2002, 2005). The asymptotic approach used in our investigation is similar in many respects to the technique applied by Vasco (2009) in a study of broadband propagation in a deformable porous medium containing a single fluid. The asymptotic approach provides semianalytic expressions for the phase velocity of a propagating disturbance and methods for the efficient solution of the governing equations. The asymptotic solution is valid in a medium with smoothly varying heterogeneity of arbitrary magnitude and thus is more general than a purely analytic solution.

METHODOLOGY

In this section, we discuss the equations governing the solid and fluid displacements in a porous medium containing two fluids. We also outline an asymptotic methodology that can provide a semi-analytic solution of the governing equations. As indicated below, the lowest-order terms in the asymptotic series produce equations for the phase velocities of the various modes of propagation.

The governing equations

Consider the case in which two fluid phases are present in the pore space of the solid matrix. The porosity of the material is denoted by ϕ , and the saturations of fluids one and two are denoted by S_1 and S_2 , respectively. The two phases are assumed to fill the entire pore space; hence, the saturations sum to unity: $S_1 + S_2 = 1$. For the time interval of interest, the elements of the porous matrix behave elastically, but the components of the fluid are described by the constitutive law for a Newtonian liquid. The fluids are assumed to behave immiscibly and one fluid can block the flow of the other. Therefore, each fluid obeys the two-phase version of Darcy's law (de Marsily, 1986), in which the flow velocity of the i th fluid relative to the solid matrix $\dot{\mathbf{w}}_i$ is proportional to the gradient of the fluid pressure:

$$\dot{\mathbf{w}}_i = -\frac{k_{r_i}k}{\mu_i} \nabla P_i, \quad (1)$$

where $k_{r_i}(S_i)$ is the relative permeability of the i th phase, k is the absolute permeability, μ_i is the fluid viscosity, and P_i is the fluid pressure. The relative permeability $k_{r_i}(S_i)$ is a function of the saturation of i th fluid phase and provides a measure of the ability of the other fluid phase present in the pore space to block the flow.

An important point is that although we are modeling the propagation of a transient disturbance in the fluid-filled porous solid, disturbance is not to be identified with the continuous flow of the fluid. Rather, the disturbance is associated with the propagation of a wave in the poroelastic medium. The wave typically will propagate much faster than any advancing fluid-saturation front. When modeling the two-phase fluid flow, there will be two timescales: the scale associated with the saturation change and the scale associated with the propagating elastic and pressure disturbance. We assume that one can model the actual field history incrementally, modeling any rapid transient disturbance in pressure and solid displacement using the equations derived here and modeling the saturation changes using quasi-static two-phase flow. As in a loosely coupled approach to modeling deformation and flow (Minkoff et al., 2003, 2004), one can introduce feedback between the solution to the poroelastic equations derived here and the reservoir simulator used to model

the long-term saturation changes. This should become clearer after we introduce the full set of coupled equations for two-phase flow.

The conservation equations

The approach used in this section is a straightforward generalization of the method of averaging. This technique, developed for a single fluid phase by Bear et al. (1984), de la Cruz and Spanos (1985), and Pride et al. (1992), is generalized to two-phase flow by Tuncay (1995) and Tuncay and Corapcioglu (1996, 1997). As in the case of a single fluid, one averages the microscopic conservation equations for the elastic solid matrix and the Newtonian fluids, making use of Slattery's (1968, 1981) theorem. The application of Slattery's theorem to the conservation equations results in governing equations for the displacements in the solid phase \mathbf{u}_s and in the fluid phases \mathbf{u}_i , $i = 1, 2$:

$$\alpha_s \rho_s \frac{\partial \dot{\mathbf{u}}_s}{\partial t} = \alpha_s \nabla \cdot \boldsymbol{\sigma}_s - \mathbf{d}_1 - \mathbf{d}_2 \quad (2)$$

and

$$\alpha_i \rho_i \frac{\partial \dot{\mathbf{u}}_i}{\partial t} = \alpha_i \nabla \cdot \boldsymbol{\sigma}_i + \mathbf{d}_i. \quad (3)$$

The dots over the displacement vectors denote the derivative with respect to time. Note that the summation convention, summation over repeated indices, is not used in this paper. In an effort to keep the presentation compact, we are representing the two equations for the fluid phases by a single indexed equation (equation 3), allowing i to take the values 1 and 2 for the respective fluid phases. The index notation, introduced above, will be implemented in much of this paper. In equations 2 and 3, the parameter α_s is the volume fraction of the solid phase, and the parameter α_i is the volume fraction of the i th fluid phase. Note that the volume fraction of the fluid phase may be written in terms of the porosity ϕ and the fluid saturation as $\alpha_i = \phi S_i$. The solid and fluid densities are denoted by ρ_s and ρ_i , respectively. The quantities $\boldsymbol{\sigma}_s$ and $\boldsymbol{\sigma}_i$ are the stress tensors associated with the solid and fluid phases. Explicit expressions for the stress tensors, in terms of the solid and fluid displacements, are given in Appendix A. The vectors \mathbf{d}_1 and \mathbf{d}_2 , referred to as the momentum transfer or interaction terms, represent drag forces from the interaction of the solid and fluids within the porous medium (Pride et al., 1993).

Pride et al. (1992) argue that the drag force can be expressed in the form

$$\mathbf{d}_i = \alpha_i \mathbf{N} \mathbf{f}_i, \quad (4)$$

where \mathbf{f}_i is the macroscopic applied force vector and \mathbf{N} is a dimensionless tensor operator independent of \mathbf{f}_i . For an isotropic medium,

$$\mathbf{N} = \nu \mathbf{I}, \quad (5)$$

where, in the most general setting, ν is an integro-differential operator. According to Pride et al. (1992, 1993), the three primary macroscopic forces influencing the motion of the fluids are a pressure gradient due to a spatially varying flow field, the relative motion of the elastic solid frame and the fluid, and fluid body forces. One can think of ν as a convolutional operator or, in the frequency domain, as a term that depends upon the frequency ω . Thus, \mathbf{N} can

change the nature of the differential operators in \mathbf{f}_i . As shown by [Pride et al. \(1992\)](#), by substituting \mathbf{d}_i into the fluid equation for the i th phase, one arrives at a specific form for \mathbf{d}_i :

$$\mathbf{d}_i = \alpha_i \nu \mathbf{f}_i = \rho_i \alpha_i \nu (1 + \nu)^{-1} \frac{\partial \dot{\mathbf{w}}_i}{\partial t}, \quad (6)$$

where $\dot{\mathbf{w}}_i$ is the flow velocity of fluid i , given in equation 1. The flow velocity of the fluid is measured relative to the position of the solid, given by $\dot{\mathbf{w}}_i = \dot{\mathbf{u}}_i - \dot{\mathbf{u}}_s$. The quantity $(1 + \nu)^{-1}$, termed the dynamic tortuosity by [Johnson et al. \(1987\)](#), controls how much relative fluid flow occurs in response to applied forces. In the case of simplified pore models, analytic methods can be used to calculate $(1 + \nu)^{-1}$ explicitly ([Johnson et al., 1987](#); [Pride et al., 1993](#)). We can substitute the expressions for \mathbf{d}_i , equation 6, into the macroscopic equations for linear momentum (equations 2 and 3). The resulting governing equations are

$$\alpha_s \rho_s \frac{\partial \dot{\mathbf{u}}_s}{\partial t} = \alpha_s \nabla \cdot \boldsymbol{\sigma}_s - D_1 \frac{\partial \dot{\mathbf{w}}_1}{\partial t} - D_2 \frac{\partial \dot{\mathbf{w}}_2}{\partial t}, \quad (7)$$

$$\alpha_i \rho_i \frac{\partial \dot{\mathbf{u}}_i}{\partial t} = \alpha_i \nabla \cdot \boldsymbol{\sigma}_i + D_i \frac{\partial \dot{\mathbf{w}}_i}{\partial t}, \quad (8)$$

where

$$D_i = \rho_i \alpha_i \nu (1 + \nu)^{-1}. \quad (9)$$

Adding and subtracting $\alpha_i \rho_i$ multiplied by the partial derivative of $\dot{\mathbf{u}}_s$ with respect to time from the left side of equation 8 produces the following system of equations in \mathbf{u}_s and \mathbf{w}_i :

$$\alpha_s \rho_s \frac{\partial \dot{\mathbf{u}}_s}{\partial t} + D_1 \frac{\partial \dot{\mathbf{w}}_1}{\partial t} + D_2 \frac{\partial \dot{\mathbf{w}}_2}{\partial t} = \alpha_s \nabla \cdot \boldsymbol{\sigma}_s \quad (10)$$

$$\alpha_i \rho_i \frac{\partial \dot{\mathbf{u}}_s}{\partial t} + (\alpha_i \rho_i - D_i) \frac{\partial \dot{\mathbf{w}}_i}{\partial t} = \alpha_i \nabla \cdot \boldsymbol{\sigma}_i, \quad (11)$$

three vector differential equations for the three unknown vectors \mathbf{u}_s , \mathbf{w}_1 , and \mathbf{w}_2 . By combining these three equations with the expressions for the stress tensors (see Appendix A) and appropriate boundary conditions, we can solve for the displacement of each phase.

There are advantages to writing the equations in the frequency domain by applying the Fourier or the Laplace transform ([Bracewell, 1978](#)). One advantage is that the time derivatives reduce to multiplication of the transformed variables by the frequency ω . This removes the time derivatives from the equations, leading to a system of equations containing only spatial derivatives. Furthermore, the convolutional operator is converted to multiplication by some function of the frequency ω . Applying the Fourier transform to each of the three equations, we can write equations 10 and 11 in the frequency domain:

$$\nu_s \mathbf{U}_s + \xi_1 \mathbf{W}_1 + \xi_2 \mathbf{W}_2 + \alpha_s \nabla \cdot \boldsymbol{\Sigma}_s = 0, \quad (12)$$

$$\nu_1 \mathbf{U}_s + \Gamma_1 \mathbf{W}_1 + \alpha_1 \nabla \cdot \boldsymbol{\Sigma}_1 = 0, \quad (13)$$

$$\nu_2 \mathbf{U}_s + \Gamma_2 \mathbf{W}_2 + \alpha_2 \nabla \cdot \boldsymbol{\Sigma}_2 = 0, \quad (14)$$

where we now write the fluid equations explicitly. In these three equations, $\boldsymbol{\Sigma}$ denotes the stress tensor transformed into the frequency domain, and we define

$$\nu_s = \alpha_s \rho_s \omega^2, \quad (15)$$

$$\nu_i = \alpha_i \rho_i \omega^2, \quad (16)$$

$$\xi_i = \alpha_i \rho_i \nu (1 + \nu)^{-1} \omega^2, \quad (17)$$

and

$$\Gamma_i = \alpha_i \rho_i [1 - \nu(1 + \nu)^{-1}] \omega^2 \quad (18)$$

for $i = 1, 2$.

To finish the statement of the governing equations, we need expressions for the divergence of the stress tensors in terms of the solid and fluid displacements. The specification of the solid and fluid stress tensors, based upon a reformulation of the work of [Tuncay and Corapcioglu \(1997\)](#), is given in Appendix A. Fourier transforming the expressions for the solid and fluid stress tensors given by equations A-24, A-25, and A-26, we can substitute them into equations 12, 13, and 14 to arrive at

$$\begin{aligned} & \nabla \cdot \left[G_m \left(\nabla \mathbf{U}_s + \nabla \mathbf{U}_s^T - \frac{2}{3} \nabla \cdot \mathbf{U}_s \mathbf{I} \right) \right] \\ & + \nabla (K_u \nabla \cdot \mathbf{U}_s + C_{s1} \nabla \cdot \mathbf{W}_1 + C_{s2} \nabla \cdot \mathbf{W}_2) \\ & + \nu_s \mathbf{U}_s + \xi_1 \mathbf{W}_1 + \xi_2 \mathbf{W}_2 = 0, \end{aligned} \quad (19)$$

$$\begin{aligned} & \nabla (C_{1s} \nabla \cdot \mathbf{U}_s + M_{11} \nabla \cdot \mathbf{W}_1 + M_{12} \nabla \cdot \mathbf{W}_2) \\ & + \nu_1 \mathbf{U}_s + \Gamma_1 \mathbf{W}_1 = 0, \end{aligned} \quad (20)$$

$$\begin{aligned} & \nabla (C_{2s} \nabla \cdot \mathbf{U}_s + M_{21} \nabla \cdot \mathbf{W}_1 + M_{22} \nabla \cdot \mathbf{W}_2) \\ & + \nu_2 \mathbf{U}_s + \Gamma_2 \mathbf{W}_2 = 0, \end{aligned} \quad (21)$$

where the coefficients of these equations are given at the end of Appendix A. Note that the coefficients depend upon the properties of the components of the medium, the saturations of the fluids S_1 and S_2 , and the capillary pressure function P_{cap} that is determined by the pressure difference in the two fluids (see equation A-4). Also, the parameter ν depends upon the flow properties of the medium and thus upon the medium permeability. For example, as indicated in the Applications section, for the model considered by [Tuncay and Corapcioglu \(1996\)](#), ν is given by

$$\nu = \frac{C_i}{C_i + \omega \alpha_i \rho_i i}, \quad (22)$$

where C_i is given by

$$C_1 = \frac{\phi^2 S_1^2 \mu_1}{k k_{r1}}, \quad (23)$$

$$C_2 = \frac{\phi^2 S_2^2 \mu_2}{k k_{r2}} \quad (24)$$

for Darcy flow.

The set of equations 19–21 is of the same general form as the governing equations for displacements in a porous media saturated by a single fluid (Pride, 2005; Vasco, 2009). There are three extra terms (those involving \mathbf{W}_2) in the first two equations (19 and 20) and one additional equation (21) governing the evolution of the second fluid phase.

An asymptotic analysis of the governing equations and semianalytic expressions for the phase

The three expressions, equations 19–21, represent a formidable set of coupled vector differential equations. Because the coefficients are functions of the spatial variables and the frequency, a closed-form, analytic solution is generally not possible. Furthermore, the equations govern both elastic deformation and diffusive fluid flow, covering a range of spatial and temporal scales. Thus, even numerical methods for solving these equations can encounter difficulties due to the wide range of scales. It is possible to gain some insight and to develop a semianalytic solution to the coupled equations by means of an asymptotic expression. The solution will be valid for a medium in which the heterogeneity is smoothly varying.

In Appendix B, we use the method of multiple scales (Whitham, 1974; Anile et al., 1993) to obtain a set of equations that can be used to determine the phase of a disturbance propagating in a heterogeneous porous medium containing two fluids. The technique has been applied to a number of problems (Korsunsky, 1997), and a variant of the technique has been used to rederive the governing equations for poroelasticity (Burrige and Keller, 1981). The method of multiple scales was used recently to construct a solution for coupled deformation and flow in a heterogeneous poroelastic medium saturated by a single fluid (Vasco, 2008, 2009). Furthermore, it has been applied to nonlinear problems involving fluid flow, such as flow in a heterogeneous medium with pressure-sensitive properties (Vasco and Minkoff, 2009) and multiphase fluid flow involving large saturation changes (Vasco, 2011).

Asymptotic expressions for displacements

There are several ways to motivate an asymptotic treatment of the governing equations 19–21. For example, one might adopt an expansion in powers of the frequency ω and consider solutions for which ω is large. However, because the coefficients contain complicated expressions in frequency and because of the diffusive and wavelike behaviors contained in the governing equations, it is best not to make specific assumptions regarding the frequency. An alternative approach is provided by the method of multiple scales, which is based upon a separation of length scales (Anile et al., 1993; Korsunsky, 1997). In particular, because we are interested in modeling propagation in a smoothly varying medium, we assume that the scale length of the heterogeneity is much greater than the scale length of the disturbance. The scale length of the disturbance, which we denote by l , is the length over which a field, such as the fluid

pressure or the displacement of the porous matrix, varies from the background value to the value associated with the disturbance. The scale length of the heterogeneity is denoted by L , and it is assumed that L is much larger than l . Thus, the ratio $\varepsilon = l/L$ is assumed to be much smaller than one. In the method of multiple scales, an asymptotic solution is constructed in terms of the ratio ε . The first step in this approach involves transforming the spatial scale from physical coordinates \mathbf{x} to slow coordinates, denoted by \mathbf{X} , where

$$\mathbf{X} = \varepsilon \mathbf{x}. \quad (25)$$

Representing the solution in terms of the slow coordinates \mathbf{X} introduces an implicit dependence on the scale variable ε . Because the scale parameter is assumed to be small, we can represent the solution as a power series in ε :

$$\mathbf{U}_s(\mathbf{X}, \omega, \theta) = e^{i\theta} \sum_{n=0}^{\infty} \varepsilon^n \mathbf{U}_s^n(\mathbf{X}, \omega), \quad (26)$$

$$\mathbf{W}_i(\mathbf{X}, \omega, \theta) = e^{i\theta} \sum_{n=0}^{\infty} \varepsilon^n \mathbf{W}_i^n(\mathbf{X}, \omega), \quad (27)$$

where the superscript n on \mathbf{U}_s^n and \mathbf{W}_i^n denotes additional terms in the summation and not exponents. The function $\theta(\mathbf{x}, \omega)$ is referred to as the local phase and is related to the kinematics of the propagating disturbance. As noted by Anile et al. (1993, p. 50), the local phase is a fast or rapidly varying quantity. Because ε is small — less than one — only the first few terms of the power series are significant. The series 26 and 27 are in the form of generalized plane-wave expansions of $\mathbf{U}_s(\mathbf{X}, \omega, \theta)$ and $\mathbf{W}_i(\mathbf{X}, \omega, \theta)$, similar to that used in modeling electromagnetic and elastic waves (Friedlander and Keller, 1955; Luneburg, 1966; Kline and Kay, 1979; Aki and Richards, 1980; Chapman, 2004).

The coordinate transformation 25 has implications for the spatial derivatives in the governing equations 19–21. For example, using the chain rule, we can rewrite the partial derivative of the solid displacement \mathbf{U}_s with respect to the spatial variable x_i as

$$\frac{\partial \mathbf{U}_s}{\partial x_i} = \frac{\partial X_i}{\partial x_i} \frac{\partial \mathbf{U}_s}{\partial X_i} + \frac{\partial \theta}{\partial x_i} \frac{\partial \mathbf{U}_s}{\partial \theta}. \quad (28)$$

Hence, making use of equation 25,

$$\frac{\partial \mathbf{U}_s}{\partial x_i} = \varepsilon \frac{\partial \mathbf{U}_s}{\partial X_i} + \frac{\partial \theta}{\partial x_i} \frac{\partial \mathbf{U}_s}{\partial \theta} \quad (29)$$

(Anile et al., 1993). Thus, the differential operators, which are defined in terms of the partial derivatives with respect to the spatial coordinates, are likewise written as

$$\nabla \mathbf{U}_s = \varepsilon \nabla_{\mathbf{X}} \mathbf{U}_s + \nabla \theta \frac{\partial \mathbf{U}_s}{\partial \theta}, \quad (30)$$

where $\nabla_{\mathbf{X}}$ denotes the gradient with respect to the components of the slow variables \mathbf{X} .

To derive an asymptotic solution, we rewrite the differential operators in the governing equations 19–21 in terms of the slow coordinates \mathbf{X} . We then substitute the power series representations 26

and 27 for \mathbf{U}_s and \mathbf{W}_i , producing three equations with terms of various orders in ε . Because ε is assumed to be much smaller than one, we consider terms of the lowest order in ε . The procedure is outlined in Appendix B, where terms of order $\varepsilon^0 \sim 1$ are presented. In the subsections that follow, we discuss these terms in greater detail, deriving explicit expressions for the phase $\theta(\mathbf{x}, \omega)$.

Before delving into the details of the expressions for the phase, we should comment as to what constitutes a smoothly varying medium. As mentioned above, a medium is smoothly varying if the scale length of the heterogeneity is much larger than the length scale of the propagating disturbance. However, the length scale of the disturbance will depend upon its frequency content. Thus, there is an implicit dependence of the scale length upon frequency and the smoothness of a medium will depend upon the frequency under consideration.

Terms of zeroth-order: The phase of the disturbance

The zeroth-order terms are presented in Appendix B, equations B-14 and B-15. These equations can be collected into the matrix equation

$$\begin{pmatrix} \alpha \mathbf{I} - \beta \mathbf{II} \cdot \mathbf{I} & \xi_1 \mathbf{I} - C_{s1} \mathbf{II} \cdot \mathbf{I} & \xi_2 \mathbf{I} - C_{s2} \mathbf{II} \cdot \mathbf{I} \\ \nu_1 \mathbf{I} - C_{1s} \mathbf{II} \cdot \mathbf{I} & \Gamma_1 \mathbf{I} - M_{11} \mathbf{II} \cdot \mathbf{I} & -M_{12} \mathbf{II} \cdot \mathbf{I} \\ \nu_2 \mathbf{I} - C_{2s} \mathbf{II} \cdot \mathbf{I} & -M_{21} \mathbf{II} \cdot \mathbf{I} & \Gamma_2 \mathbf{I} - M_{22} \mathbf{II} \cdot \mathbf{I} \end{pmatrix} \times \begin{pmatrix} \mathbf{U}_s^0 \\ \mathbf{W}_1^0 \\ \mathbf{W}_2^0 \end{pmatrix} = \begin{pmatrix} \mathbf{0} \\ \mathbf{0} \\ \mathbf{0} \end{pmatrix}, \quad (31)$$

where $\mathbf{I} = \nabla \theta$ is the local phase gradient,

$$\alpha = \nu_s - G_m l^2, \quad (32)$$

$$\beta = K_u + \frac{1}{3} G_m, \quad (33)$$

l is the magnitude of the local phase gradient vector \mathbf{I} , $\mathbf{II} \cdot \mathbf{I}$ is a dyadic formed by the outer product of the vector \mathbf{I} (Ben-Menahem and Singh, 1981; Chapman, 2004) (see equation B-11), and the coefficients are given in (equations 15–18) and in Appendix A. Alternatively, one may think of the dyadic \mathbf{II} as the vector outer product \mathbf{II}^T , where \mathbf{I}^T signifies the transpose of \mathbf{I} , converting the column vector \mathbf{I} to the row vector \mathbf{I}^T .

The system of equation 31 has a nontrivial solution if and only if the determinant of the coefficient matrix vanishes (Noble and Daniel, 1977, p. 203). For a given set of coefficients, the determinant of the matrix is a polynomial in the components of the vector \mathbf{I} . Given that the components of the vector \mathbf{I} are the elements of the gradient of the phase θ , the polynomial equation is also a partial differential equation for the phase function. This nonlinear differential equation is the eikonal equation associated with propagation in a porous medium saturated with two fluid phases (Kravtsov and Orlov, 1990; Chapman, 2004). Although we could attempt to find the roots of the ninth-order polynomial equation directly, that approach would involve some rather lengthy algebra. In Appendix C, we describe an approach based upon the eigenvectors of the system of equation 31. In that approach, the modes of propagation are

partitioned into longitudinal displacements (displacement in the direction of \mathbf{I}), and transverse displacements (displacement in a direction perpendicular to \mathbf{I}). The results of that approach are discussed next.

Longitudinal displacements

As shown in Appendix C, for the longitudinal modes of propagation, the condition that equation 31 has a nontrivial solution is

$$\det \begin{pmatrix} \nu_s - H l^2 & \xi_1 - C_{s1} l^2 & \xi_2 - C_{s2} l^2 \\ \nu_1 - C_{1s} l^2 & \Gamma_1 - M_{11} l^2 & -M_{12} l^2 \\ \nu_2 - C_{2s} l^2 & -M_{21} l^2 & \Gamma_2 - M_{22} l^2 \end{pmatrix} = 0, \quad (34)$$

where we have used the definitions 32 and 33 and defined the parameter H as

$$H = K_u + \frac{4}{3} G_m. \quad (35)$$

Equation 34 is a cubic equation in l^2 , the square of the magnitude of the slowness vector \mathbf{I} . Solving this cubic equation for l^2 allows one to determine the permissible modes of longitudinal displacement.

Equation 34 is much more complicated than the single-phase constraint, which is the determinant of a 2×2 matrix (Vasco, 2009). Therefore, one must exercise care when calculating the determinant in equation 34. This calculation is given in some detail in Appendix D, where we apply, in a recursive fashion, a rule for computing the determinant of a matrix whose columns are sums. As shown in Appendix D, we can write the cubic equation for $s = l^2$ as

$$Q_3 s^3 - Q_2 s^2 + Q_1 s - Q_0 = 0, \quad (36)$$

where the coefficients are given by

$$Q_3 = \det \begin{pmatrix} H & C_{s1} & C_{s2} \\ C_{1s} & M_{11} & M_{12} \\ C_{2s} & M_{21} & M_{22} \end{pmatrix}, \quad (37)$$

$$Q_2 = \det \begin{pmatrix} \nu_s & C_{s1} & C_{s2} \\ \nu_1 & M_{11} & M_{12} \\ \nu_2 & M_{21} & M_{22} \end{pmatrix} + \det \begin{pmatrix} H & \xi_1 & C_{s2} \\ C_{1s} & \Gamma_1 & M_{12} \\ C_{2s} & 0 & M_{22} \end{pmatrix} + \det \begin{pmatrix} H & C_{s1} & \xi_2 \\ C_{1s} & M_{11} & 0 \\ C_{2s} & M_{21} & \Gamma_2 \end{pmatrix}, \quad (38)$$

$$Q_1 = \det \begin{pmatrix} \nu_s & \xi_1 & C_{s2} \\ \nu_1 & \Gamma_1 & M_{12} \\ \nu_2 & 0 & M_{22} \end{pmatrix} + \det \begin{pmatrix} \nu_s & C_{s1} & \xi_2 \\ \nu_1 & M_{11} & 0 \\ \nu_2 & M_{21} & \Gamma_2 \end{pmatrix} + \det \begin{pmatrix} H & \xi_1 & \xi_2 \\ C_{1s} & \Gamma_1 & 0 \\ C_{2s} & 0 & \Gamma_2 \end{pmatrix}, \quad (39)$$

$$Q_0 = \det \begin{pmatrix} \nu_s & \xi_1 & \xi_2 \\ \nu_1 & \Gamma_1 & 0 \\ \nu_2 & 0 & \Gamma_2 \end{pmatrix}. \quad (40)$$

The roots of the cubic equation 36 determine the value of l , the magnitude of the phase gradient vector $\mathbf{l} = \nabla\theta$. To find the roots, we first put equation 36 in a canonical form by dividing through by Q_3 :

$$s^3 - \frac{Q_2}{Q_3}s^2 + \frac{Q_1}{Q_3}s - \frac{Q_0}{Q_3} = 0. \quad (41)$$

Or, if we define the coefficients

$$\Upsilon_2 = \frac{Q_2}{Q_3}, \quad (42)$$

$$\Upsilon_1 = \frac{Q_1}{Q_3}, \quad (43)$$

and

$$\Upsilon_0 = \frac{Q_0}{Q_3}, \quad (44)$$

we can write equation 41 as

$$s^3 - \Upsilon_2 s^2 + \Upsilon_1 s - \Upsilon_0 = 0. \quad (45)$$

Note that, in dividing by Q_3 , we are assuming the determinant of the coefficient array is not zero. The determinant Q_3 vanishes if any of the rows of the coefficients of the l^2 terms in the determinant 34 are linear dependent. This can occur if the properties of the two fluids are similar and it becomes difficult to distinguish between the fluids.

The solution of the cubic equation 45 can be written explicitly as a function of the coefficients (Stahl, 1997, p. 47). We begin by defining

$$\eta = \frac{1}{3}(\Upsilon_2)^2 - \Upsilon_1 \quad (46)$$

and

$$\gamma = \frac{2}{27}(\Upsilon_2)^3 - \frac{1}{3}\Upsilon_1\Upsilon_2 + \Upsilon_0. \quad (47)$$

Furthermore, if we define the parameter ζ as

$$\zeta = \frac{4}{27\gamma^2}\eta^3, \quad (48)$$

then we can write the solution of equation 45 in the form

$$s = l^2 = \sqrt[3]{\frac{\gamma}{2} \left[1 \pm \sqrt{1 - \zeta} \right]} - \frac{1}{3} \frac{\eta}{\sqrt[3]{\frac{\gamma}{2} \left[1 \pm \sqrt{1 - \zeta} \right]}} + \frac{\Upsilon_2}{3}, \quad (49)$$

an expression for the squared phase gradient magnitude in terms of the medium parameters. Although the first term in equation 49 shares a formal similarity to the phase of a disturbance propagating in a porous medium containing a single liquid (Vasco, 2009), the overall expression is decidedly more complicated.

Because l is the magnitude of the phase gradient vector $\mathbf{l} = \nabla\theta$, we can use equation 49 to formulate a differential equation for θ :

$$\begin{aligned} \nabla\theta \cdot \nabla\theta &= \sqrt[3]{\frac{\gamma}{2} \left[1 \pm \sqrt{1 - \zeta} \right]} - \frac{1}{3} \frac{\eta}{\sqrt[3]{\frac{\gamma}{2} \left[1 \pm \sqrt{1 - \zeta} \right]}} + \frac{\Upsilon_2}{3}, \end{aligned} \quad (50)$$

which is an eikonal equation for the phase of the propagating disturbance (Kravtsov and Orlov, 1990). Equation 50 provides all of the information necessary for modeling the kinematics, i.e., the traveltime, of the propagating disturbance. For example, one may solve the nonlinear partial differential equation 50 numerically, using a fast marching method (Sethian, 1985, 1999), which was introduced to seismology by Vidale (1988). The fast marching approach has proven to be stable, even in the presence of rapid changes in medium properties. Or one may use the method of characteristics (Courant and Hilbert, 1962) to derive a related set of ordinary differential equations, the ray equations (Anile et al., 1993; Chapman, 2004) that can be solved numerically (Press et al., 1992).

Transverse displacements

Now we consider the case in which the displacements are perpendicular to the propagation direction. In that situation, the eigenvector is given by the solution of an equation similar to equation C-5 in Appendix C:

$$\mathbf{\Gamma} \mathbf{e}^\perp = \lambda^\perp \mathbf{e}^\perp = 0, \quad (51)$$

where λ^\perp is the associated eigenvalue. Invoking similar arguments to those used in the analysis in Appendix C but tailored to transverse displacements, we can show that the vanishing of the determinant of the matrix $\mathbf{\Gamma}$ reduces to

$$\det \begin{pmatrix} \nu_s - G_m l^2 & \xi_1 & \xi_2 \\ \nu_1 & \Gamma_1 & 0 \\ \nu_2 & 0 & \Gamma_2 \end{pmatrix} = 0, \quad (52)$$

a quadratic equation for l , whose coefficients depend upon the frequency and the properties of the porous medium and the fluids. The determinant 52 is a straightforward calculation, resulting in the quadratic equation

$$\Gamma_1 \Gamma_2 G_m l^2 - \nu_s \Gamma_1 \Gamma_2 + \nu_1 \xi_1 \Gamma_2 + \nu_2 \Gamma_1 \xi_2 = 0, \quad (53)$$

which can be solved for l :

$$l = \pm \sqrt{\frac{\Gamma_1 \Gamma_2 \nu_s - \xi_1 \Gamma_2 \nu_1 - \Gamma_1 \xi_2 \nu_2}{\Gamma_1 \Gamma_2 G_m}}. \quad (54)$$

Thus, there is a single solution for phase gradient magnitude associated with the transverse mode of displacement. The different signs indicate propagation in the forward and reverse directions along **I**.

The expression for l in the case of transverse displacements (equation 54) is much simpler than that for longitudinal displacements (equation 49). We shall rewrite it to bring out some similarities to the expression for a single fluid (Vasco, 2009). If we factor out $\Gamma_1\Gamma_2$ and use the definitions for ν_s, ν_1 , and ν_2 , equation 54 can be written as

$$l = \pm\omega\sqrt{\frac{\alpha_s\rho_s - \frac{\alpha_1\xi_1}{\Gamma_1}\rho_1 - \frac{\alpha_2\xi_2}{\Gamma_2}\rho_2}{G_m}} \quad (55)$$

or as

$$l = \pm\omega\sqrt{\frac{(1-\phi)\rho_s - \phi\rho_f}{G_m}}, \quad (56)$$

where

$$\rho_f = \frac{\xi_1}{\Gamma_1}S_1\rho_1 + \frac{\xi_2}{\Gamma_2}S_2\rho_2 \quad (57)$$

is a weighted fluid density whose weights are a function of frequency through the dependence upon ν . Equation 56 is a direct modification of the expression for the slowness of an elastic shear wave. Equation 56 generalizes the expression for wave propagation in a porous medium saturated by a single fluid phase (Pride, 2005; Vasco, 2009), where one has

$$l = \pm\omega\sqrt{\frac{\rho_s - \frac{\rho_f}{\bar{\rho}}\rho_f}{G_m}}, \quad (58)$$

where $\bar{\rho}$ is $i\mu_f/\omega k$ for a fluid of density ρ_f and viscosity μ_f .

APPLICATIONS

Comparison with previous studies

Here we compare our results with Tuncay and Corapcioglu's (1996) and Lo et al.'s (2005) studies of wave propagation in a homogeneous porous medium containing two fluid phases and with experimental data (Murphy, 1982). First, in the case of transverse displacements, we establish the equivalence of our expression for the phase velocity to that of Tuncay and Corapcioglu (1996) when the medium is homogeneous and when we define ν in a particular fashion. Second, we compare numerical predictions of complex velocities for the three longitudinal modes of propagation in a porous medium saturated by two fluid phases. We compare predictions derived using our formulation with those by Tuncay and Corapcioglu (1996) and Lo et al. (2005). Finally, we calculate the primary longitudinal and the transverse velocities for the porous Massilon sandstone partially saturated by water, as described in Murphy (1982).

Transverse (shear) displacements

It is simplest to begin our comparisons with the expression for the phase gradient magnitude of the shear component, given by

equation 54. Before we begin, it must be noted that our phase function θ , introduced in the power series 26 and 27, is defined slightly differently from the conventional use in seismic applications. Specifically, we include the frequency term ω as part of θ . Thus, our definition of l will contain an additional ω factor, and the square of the phase velocity will be given by

$$c^2 = \frac{\omega^2}{l^2}. \quad (59)$$

Let us begin with an expression for $1/l^2$, where l is given by equation 54:

$$\frac{1}{l^2} = \frac{\Gamma_1\Gamma_2G_m}{\Gamma_1\Gamma_2\nu_s - \xi_1\Gamma_2\nu_1 - \Gamma_1\xi_2\nu_2}. \quad (60)$$

The coefficients are given by expressions 15–18. However, the coefficients $\Gamma_1, \Gamma_2, \xi_1$, and ξ_2 contain the operator ν , which depends upon the fluid response to applied forces (Johnson et al., 1987; Pride et al., 1993). To compare our predicted velocities with those of Tuncay and Corapcioglu (1996), we need to relate these coefficients to those used in their paper. By comparing the coefficients in their governing equations 1–3 with the coefficients in the governing equations 12–14, after accounting for the slightly different formulation and after transforming their equations to the frequency domain, we find that

$$\xi_1 = -i\omega C_1, \quad (61)$$

$$\xi_2 = -i\omega C_2, \quad (62)$$

$$\Gamma_1 = \omega^2\hat{\rho}_1 + i\omega C_1, \quad (63)$$

and

$$\Gamma_2 = \omega^2\hat{\rho}_2 + i\omega C_2, \quad (64)$$

where $\hat{\rho}_i$ is the volume averaged density, given by $\hat{\rho}_i = \alpha_i\rho_i = \phi S_i\rho_i$, and C_1 and C_2 are coefficients defined in Tuncay and Corapcioglu (1996), related to the fluid flow. The coefficients take the form

$$C_1 = \frac{\phi^2 S_1^2 \mu_1}{k k_{r1}}, \quad (65)$$

$$C_2 = \frac{\phi^2 S_2^2 \mu_2}{k k_{r2}} \quad (66)$$

for Darcy flow, where S_i is the saturation of the i th fluid, μ_i is the fluid viscosity for phase i , k is the absolute permeability, and $k_{r,i}$ is the relative permeability for fluid i . Using relationships 61–64, we can rewrite the product as

$$\Gamma_1\Gamma_2 = \omega^2[\hat{\rho}\hat{\rho}_2\omega^2 - C_1C_2 + \omega(C_1\hat{\rho}_2 + C_2\hat{\rho}_1)i], \quad (67)$$

as well as the other terms in expression 60. As a result, the square of the phase velocity c^2 can be expressed as the ratio

$$c^2 = \frac{\omega^2}{l^2} = -\frac{Y_2}{Y_1}, \quad (68)$$

where

$$Y_1 = \frac{C_1 C_2 (\hat{\rho}_s + \hat{\rho}_1 + \hat{\rho}_2) - \hat{\rho}_s \hat{\rho}_1 \hat{\rho}_2}{\omega^2} - i \frac{C_2 \hat{\rho}_1 (\hat{\rho}_s + \hat{\rho}_2) + C_1 \hat{\rho}_2 (\hat{\rho}_s + \hat{\rho}_1)}{\omega} \quad (69)$$

and

$$Y_2 = -G_m \frac{C_1 C_2 - \hat{\rho}_1 \hat{\rho}_2 \omega^2}{\omega^2} + i G_m \frac{C_2 \hat{\rho}_1 + C_1 \hat{\rho}_2}{\omega}. \quad (70)$$

These expressions agree with those of [Tuncay and Corapcioglu \(1996\)](#) for the phase velocity of the shear wave (see their equations 28–30).

Note that, using equations 17 and 61, one can derive an explicit expression for the frequency-dependent variable ν that determines the dynamic tortuosity $(1 + \nu)^{-1}$. Recall that the dynamic tortuosity controls the amount of fluid flow in response to the applied forces. The variable ν also appears in the definition of the coefficients ξ_i and Γ_i (see equations 17 and 18), which are part of the governing equations. Equating the expressions for ξ_i given in equations 17, 61, and 62, we have

$$\nu(1 + \nu)^{-1} = \left(\frac{-i}{\omega} \right) \frac{C_i}{\alpha_i \rho_i}. \quad (71)$$

Solving equation 71 for ν gives

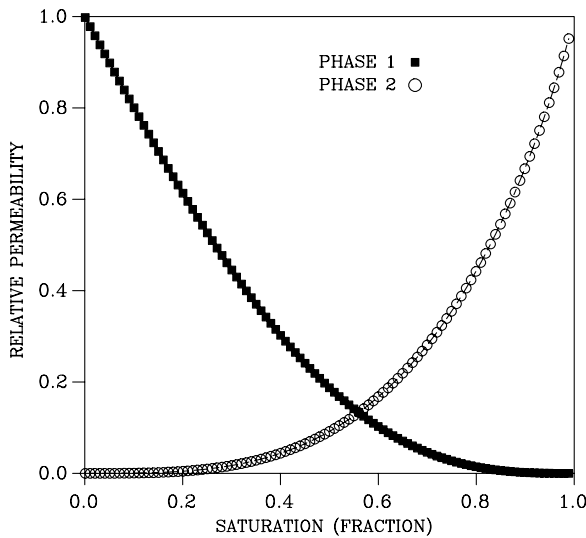


Figure 1. The relative permeability curves of [Mualem \(1976\)](#) for fluid flow in a porous medium saturated by two fluids. The curves describe the variation of the relative permeability $k_{ir}(S_i)$, the function appearing in the expressions 65 and 66 for C_1 and C_2 . The algebraic expressions for these curves are given by equations 75 and 76. Fluid 1 is the gas phase (air); fluid 2 is the liquid phase (water).

$$\nu = \frac{C_i}{C_i + \omega \alpha_i \rho_i i}, \quad (72)$$

where C_i is given by equations 65 and 66. Equation 72 indicates that ν is actually a function of the specific fluid. Thus, in the most general case, ν should vary for each fluid. This makes physical sense because the flow characteristics of each fluid can differ.

Longitudinal displacements

Although it is possible to apply the previous mathematical analysis to the longitudinal modes, that approach would be significantly more complicated. It is far simpler to proceed with a direct numerical comparison of the predictions provided by the expressions of [Tuncay and Corapcioglu \(1996\)](#) and [Lo et al. \(2005\)](#) with those from the solutions of the cubic equation 36. Because the phase velocities are generated by the cubic equation with complex coefficients given by expressions 37–40, there will be three complex longitudinal velocities in general.

A comparison with [Tuncay and Corapcioglu \(1996\)](#).—For the first comparison, with the results of [Tuncay and Corapcioglu \(1996\)](#), the poroelastic parameters for the medium are representative of the properties of the Massilon sandstone described by [Murphy \(1982\)](#). Thus, the bulk modulus K_{fr} of the frame is 1.02 GPa, the bulk modulus of the grains K_s is 35.00 GPa, shear modulus G_{fr} is 1.44 GPa, the density of the solid grains ρ_s is 2650.00 kg/m³, the intrinsic permeability of the sandstone k is 9.0×10^{-13} m², and the volume fraction of the solid phase α_s is 0.77. The two fluid phases are air (fluid 1) and water (fluid 2), with respective viscosities μ_1 and μ_2 of 18×10^{-6} and 1.0×10^{-3} Pa-s. For fluid 1 (air), the bulk modulus K_1 is 0.145 MPa and the density ρ_1 is 1.10 kg/m³. For fluid 2 (water), K_2 is 2.25 GPa and ρ_2 is 997.00 kg/m³. The capillary function P_{cap} used here (see equation A-4) was first proposed by [van Genuchten \(1980\)](#). The exact form of the capillary function is

$$P_{cap}(S_2) = -\frac{100}{\alpha} \left[\left(1 - \frac{S_2 - S_{rw}}{S_{m2} - S_{r2}} \right)^m \right]^{-n}, \quad (73)$$

where S_{r2} is the residual water saturation, taken to be 0.0, and S_{m2} is the upper limit of water saturation $m = 1 - 1/n$, where $n = 10$ and $\alpha = 0.025$. The relative permeability functions associated with the two fluids in the porous matrix, those postulated by [Mualem, 1976](#); [van Genuchten, 1980](#), are shown in Figure 1. An examination of the functions C_1 and C_2 , given by equations 65 and 66, reveals that they are singular when the relative permeabilities vanish. Thus, some care is required as the fluid saturations approach the end points of the curves shown in Figure 1. For this reason, we shall avoid those saturations at which the relative permeabilities approach zero.

The phase velocities predicted using expression 59, where l^2 is a root of the cubic equation 36, are plotted in Figure 2 along with the phase velocities predicted using the formulas of [Tuncay and Corapcioglu \(1996\)](#). The phase velocities, the real component of the complex number c , are associated with a frequency of 1000 Hz. The cubic equation predicts three complex velocities varying as a function of fluid saturation. We should note that a_{11} in expressions 21–23 of [Tuncay and Corapcioglu \(1996\)](#) should be replaced by the variable $a_{11}^* = a_{11} + 4G_{fr}/3$ for the three formulas to agree

with their previous equation 18, which contains a_{11}^* . As indicated in Figure 2, there is excellent agreement between our predicted longitudinal velocities and those given by the formulas of Tuncay and Corapcioglu (1996). The qualitative features noted by Tuncay and Corapcioglu (1996) are present in the velocities plotted in Figure 2. For example, the velocities of the first two modes of longitudinal propagation drop significantly as the water saturation decreases from one. This is due to the much higher compressibility of air compared with that of water. With further decreases in water saturation, there is a gradual increase in the phase velocities of the two modes. As noted by Tuncay and Corapcioglu (1996), the third longitudinal mode arises due to the pressure difference between the fluid phases. Thus, this phase velocity approaches zero when the fluid saturations approach fully saturated or fully unsaturated conditions because the capillary pressure vanishes when only a single fluid occupies the pore space.

The imaginary component of the phase velocity c , given by equation 59, provides a measure of the attenuation. The attenuation varies as $\exp(-c_i r)$, where c_i is the imaginary component of the phase velocity and r the radial distance from the source. In Figure 3, we plot the attenuation coefficient for the three longitudinal modes, calculated using the expressions of Tuncay and Corapcioglu (1996) and the roots of cubic equation 36. There is excellent agreement between the two approaches. The attenuation overall is quite small for the first longitudinal mode of propagation, which propagates much like an elastic wave in the solid. As noted in Tuncay and Corapcioglu (1996), the attenuation is due to energy dissipation induced by the relative motion of the fluids and the solid. Furthermore, they note that the end-point attenuation in the second mode of longitudinal propagation is determined by the kinematic viscosity, the ratio of the fluid viscosity to the fluid density. The attenuation coefficient of the third longitudinal mode of propagation is quite large and increases as the fraction of either phase becomes large. Perhaps this is due to the increased flow as the pore space is dominated by a single fluid. Also, the capillary pressure which drives this mode decreases as one phase begins to vanish, resulting in a rapidly decreasing amplitude for the third mode of propagation.

A comparison with Lo et al. (2005).—Recently, Lo et al. (2002, 2005) have followed an alternative approach in deriving the equations governing coupled poroelastic deformation and flow. Specifically, they use the mass-balance equations for the three-phase system (two fluids and one solid) coupled with a closure relation for porosity change to derive the governing equations. The resulting system of equations is similar to those given above. In particular, their stress-strain relations (given by equations 32a–32c of Lo et al. [2005]) are equivalent to our equations A-18, A-20, and A-21. The coefficients in their stress-strain relations, also denoted by a_{ij} (given by equations 30d–30j in Lo et al. [2005]), are identical to those of Tuncay and Corapcioglu (1996) and to expressions A-7–A-17. The primary differences between the equations presented here and those of Lo et al. (2005) are because of the inclusion of temperature effects and inertial coupling terms between the fluids that we do not include. Lo et al. (2005) note that their equations include inertial terms due to the differential movement between the solid and the fluids. They contrast their results with the expressions of Tuncay and Corapcioglu (1996) that do not contain such inertial terms. However, our expressions, in particular the coefficients Γ_i given

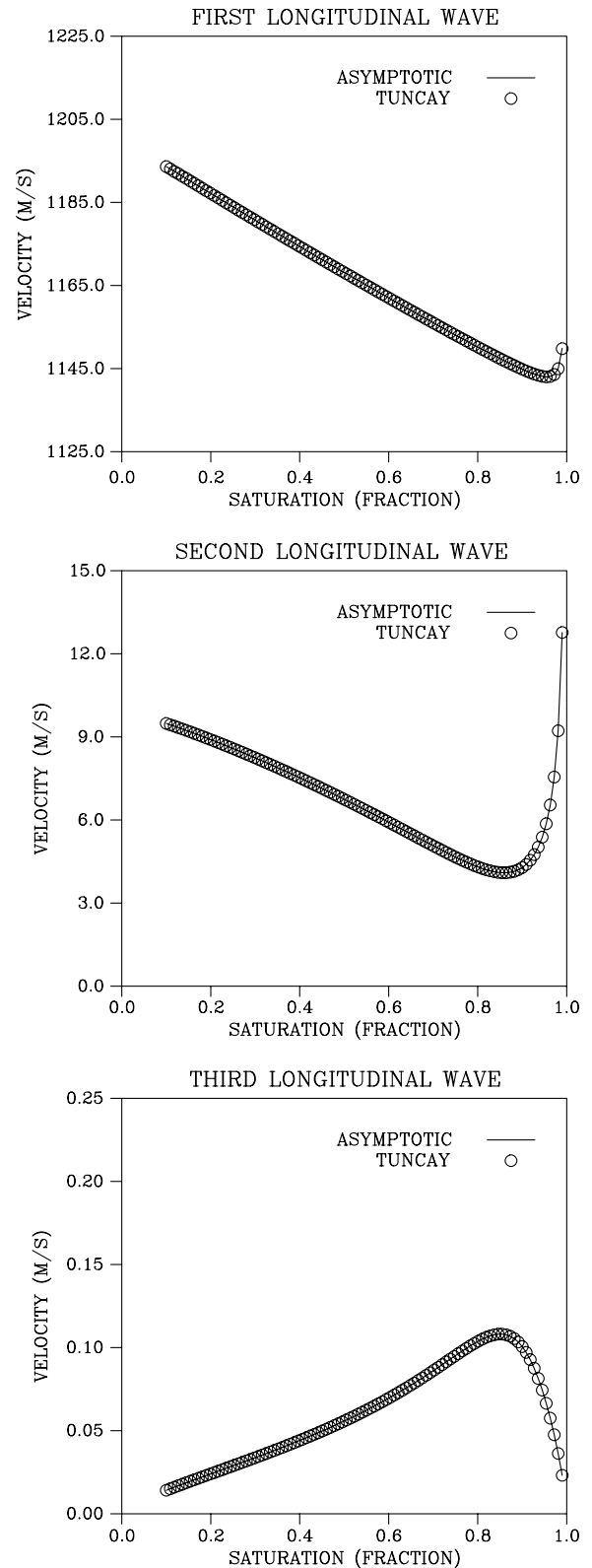


Figure 2. The three phase velocities associated with the longitudinal modes of propagation in a porous medium saturated with two fluids. The phase velocities are plotted as functions of water saturation. The frequency used in the computations was 1000 Hz. The phase velocities are determined by the real component of the roots of cubic equation 36.

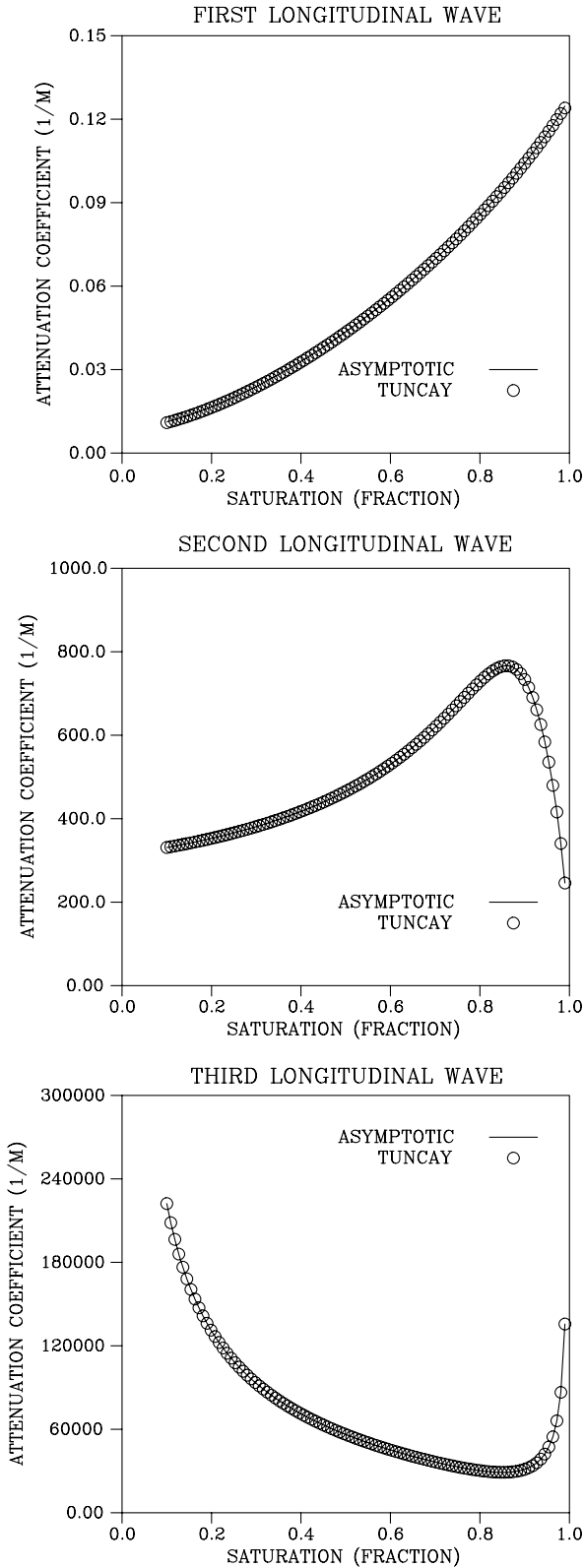


Figure 3. The attenuation of a propagating longitudinal mode of displacement, plotted as a function of water saturation. The frequency used in the computations was 1000 Hz. The attenuation is determined by the imaginary components of the three roots of cubic equation 36.

by equation 18, do contain inertial effects due to the coupling between the solid and the fluids, in the form of ω^2 terms.

For a qualitative comparison of our expressions and those of Lo et al. (2005), we have computed the three longitudinal velocities for the two simulations described in their paper. The porous solid properties are based upon experimental data for an unconsolidated Columbia fine sandy loam (Chen et al., 1999; Lo et al., 2005). The primary difference between this porous material and the sandstone described above is that the fine sandy loam is unconsolidated and hence much weaker. Thus, the bulk modulus of the rock frame K_{fr} is only 0.008 GPa, a fraction of the value of 1.02 GPa for the sandstone. Similarly, the shear modulus of the frame for the loam G_{fr} is quite low, 0.004 GPa, compared to a value of 1.44 GPa for the consolidated sandstone. Note that both materials are primarily composed of silica grains and the bulk modulus of the solid particles is 35 GPa. Therefore, we would expect quite different bulk velocities for the consolidated sandstone and the unconsolidated sandy loam.

Lo et al. (2005) consider two pairs of fluids: an air-water system, similar to that of Tuncay and Corapcioglu (1996), and an oil-water mixture. The properties of the constituents in the air-water system are similar to those used in Tuncay and Corapcioglu (1996): the bulk modulus of air is 0.145 MPa, the bulk modulus of water is 2.25 GPa, and the densities of air and water are 1.1 and 997.0 kg/m³, respectively. The viscosity of air is 18×10^{-6} Pa-s, and the viscosity of water is 0.001 Pa-s. For the oil, the bulk modulus is given by 0.57 GPa, the density is given by 762 kg/m³, and the viscosity is given by 0.00144 Pa-s. The derivative of the capillary pressure with respect to changes in saturation is given explicitly by

$$\frac{dP_{cap}}{dS_1} = \frac{\rho_2 g}{mn\chi} \left[(1 - S_1)^{-\frac{n}{n-1}} - 1 \right]^{\frac{1-m}{n}} (1 - S_1)^{-\left(\frac{2n-1}{n-1}\right)} \quad (74)$$

(Lo et al., 2005), where g is the gravitational acceleration. The quantities χ , m , and n are fitting parameters with values $\chi = 1 \text{ m}^{-1}$, $n = 2.145$, and $m = 1 - 1/n = 0.534$ for the air-water system. For the oil-water system, the parameters are given by $\chi = 2.39 \text{ m}^{-1}$, $n = 2.037$, and $m = 1 - 1/n = 0.509$ (Lo et al., 2005). This is the same model of capillary pressure put forward by van Genuchten (1980) and used above, though in a slightly different formulation (see equation 73).

The relative permeability functions are those of Mualem (1976), which were used in the previous comparison. The exact algebraic expressions are

$$k_{r1}(S_2) = (1 - S_2)^\eta [1 - (S_2)^{\frac{1}{m}}]^{2m}, \quad (75)$$

$$k_{r2}(S_2) = (S_2)^\eta \{1 - [1 - (S_2)^{\frac{1}{m}}]^m\}^2, \quad (76)$$

where η is a fitting parameter (Mualem, 1976). The fitting parameter η associated with the air-water and the oil-water mixtures is 0.5, as noted in Lo et al. (2005).

We computed the three longitudinal velocities for the air-water system and the oil-water mixture as a function of the water saturation. The velocities of the first longitudinal wave are plotted in Figure 4 for the air-water and the oil-water fluid mixtures. The

velocities are computed at a single frequency of 100 Hz for this phase. As expected, the bulk velocities for the air-water system are much lower for the unconsolidated sandy loam (on average, 100 m/s; Figure 4), than for the sandstone (between 1140 and 1200 m/s; Figure 2). In Figure 4, the velocities calculated using the expressions of Tuncay and Corapcioglu (1996) are indicated by the dashed (oil-water) and solid (air-water) lines, whereas our calculated values are indicated by the filled squares (air-water) and the open circles (oil-water). The behavior of the air-water and the oil-water systems is rather different as the saturations are varied. When the water saturation is near zero, the bulk velocities of the two systems are distinctly different, with the velocity of the oil-water mixture approximately eight times larger than the velocity of the air-water mixture. This reflects the influence of the pore fluids because the systems are saturated by two very different fluids. The velocity in the oil-water system gradually increases as the water saturation increases. This contrasts with the behavior of the air-water system in which the velocity remains nearly constant until rather high water saturation. The velocity increases dramatically when the porous medium is almost completely water saturated. The velocity increases dramatically when the porous medium is almost completely water saturated. When the material is entirely saturated by water, the velocities are nearly equal for the air-water and oil-water systems. This makes physical sense because both systems are in identical water-saturated states. However, there may be slight differences because, as noted in Lo et al. (2005), two different permeabilities are used by Chen et al. (1999) to fit the observational data. Our calculated velocities agree with those computed using the expressions of Tuncay and Corapcioglu (1996). Furthermore, the variations of the first longitudinal velocity, denoted by $P1$, agree with those of Lo et al. (2005) (see their Figure 1a).

The longitudinal mode of intermediate velocity, often referred to as the $P2$ mode, is associated with diffusive propagation in the manner of a transient pressure variation (Pride, 2005). The propagating disturbance corresponds to the out-of-phase motion of the solid and fluid mixtures (Lo et al., 2005; Pride, 2005). The disturbance is known as the slow wave in the study of wave propagation in a medium saturated with a single fluid (Pride, 2005; Vasco, 2009). In Figure 5, we plot the calculated intermediate velocities for the air-water and oil-water fluid mixtures in the sandy loam at a frequency of 100 Hz. The average velocities are much lower for this mode of propagation, on the order of 1 – 2 m/s. The computed variations (filled squares and open circles) generally agree with the predictions of Tuncay and Corapcioglu (1996) (solid and dashed lines). There is some deviation for the oil-water system at high water saturations. The estimates are of the same order as those of Lo et al. (2005). However, the exact values differ by a factor of two or more, and there are differences in the nature of the variation for the air-water system at high water saturations. As in the case of the $P1$ mode, the velocities of the two systems approach each other as the medium becomes water saturated.

The third mode of propagation $P3$, with the lowest velocity, arises from the pressure difference between the two fluid phases (Tuncay and Corapcioglu, 1996). Thus, the disturbance is the result of the presence of a second fluid in the pore space and is not observed in systems with a single fluid phase. Such a phase is extremely difficult to observe experimentally (Tuncay and Corapcioglu, 1996) due to its high attenuation and extremely low velocity. In Figure 6, we plot the calculated velocities of the $P3$ mode for the air-water and oil-water mixtures at a frequency of 100 Hz.

The velocities are extremely low, generally less than 0.1 m/s. As noted in other studies (Tuncay and Corapcioglu, 1996; Lo et al., 2005), the velocities approach zero at high and low water saturations. As in the case of the other two modes, the air-water and oil-water velocities approach a common value (in this case, zero) as the water saturation approaches one. There is general agreement

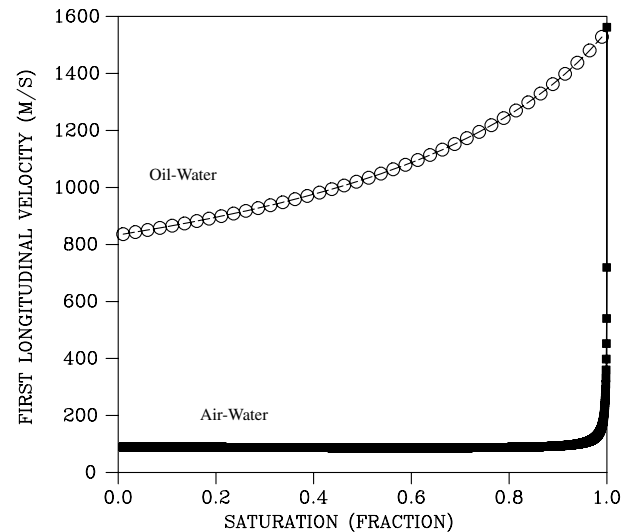


Figure 4. Velocities for the first (fastest) longitudinal mode, known as $P1$, plotted as a function of the water saturation. Two fluid mixtures are shown in this figure: an air-water mixture and an oil-water mixture. The velocities calculated using the expressions in this paper are plotted as open circles for the oil-water system and solid squares for the air-water system. In addition, the values computed using the formulas of Tuncay and Corapcioglu (1996) are plotted as a dashed line (oil-water) and a solid line (air-water).

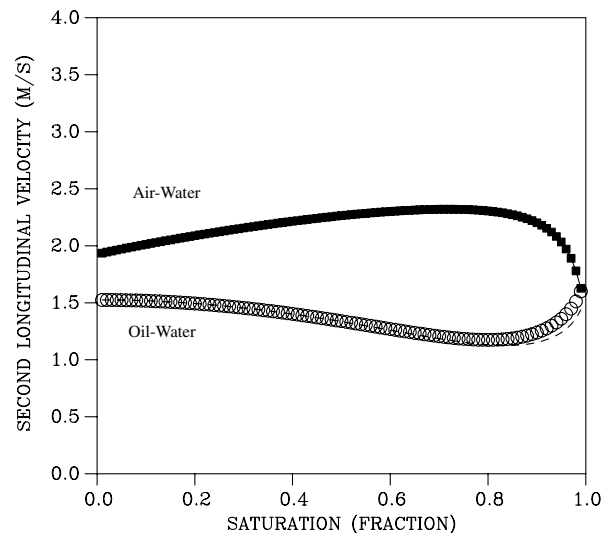


Figure 5. The velocities associated with the second or intermediate $P2$ mode of propagation, plotted as a function of water saturation. The values computed using the formulas of Tuncay and Corapcioglu (1996) are plotted as a dashed line (oil-water) and a solid line (air-water).

between our estimates and those of [Tuncay and Corapcioglu \(1996\)](#) and [Lo et al. \(2005\)](#).

The velocities of the three modes of propagation are frequency dependent. To compare the variation with frequency we have computed the velocities for three frequencies: 50, 100, and 200 Hz. In all of the computations, we only consider the air-water system. For the first longitudinal mode $P1$, as noted in [Lo et al. \(2005\)](#); (see their Figure 1a), the velocities do not change over this range of frequencies. Thus, we have not plotted the velocities because they are identical to those shown in Figure 4. In Figure 7, we plot the velocities for the intermediate model $P2$ at the three frequencies of interest. As in [Lo et al. \(2005\)](#), the velocities increase as the frequencies increase. A similar pattern of higher velocities with increasing frequency is observed for the third longitudinal mode of propagation $P3$, as shown in Figure 8.

A comparison with laboratory observations

Here, we compare data from a series of experiments by [Murphy \(1982\)](#) to predictions based upon our formulation. These and other experimental studies have shown that fluid saturations can have a significant influence upon the phase velocities of extensional (longitudinal) and rotational (transverse) waves in a sample ([Domenico, 1974, 1976; Murphy, 1982](#)). Although many laboratory experiments, such as those of [Domenico \(1974, 1976\)](#) are conducted at high frequency, the resonance bar experiments of [Murphy \(1982\)](#) span a wide frequency range, from 300 Hz to 14 kHz. In addition, a torsional pendulum technique was used to measure rotational (transverse) wave attenuation at low acoustic frequencies ([Murphy, 1982](#)). The flow experiments of [Murphy \(1982\)](#) were conducted in a sample of Massillon sandstone. The properties of this porous material are identical to those noted above for the Massillon sandstone ([Murphy, 1982; Tuncay and Corapcioglu, 1996](#)).

The relative-permeability curves used to represent the flow of the two fluids, air and water, in the sandstone are those published by [Wyckoff and Botset \(1936\)](#) and shown in Figure 9. These curves are

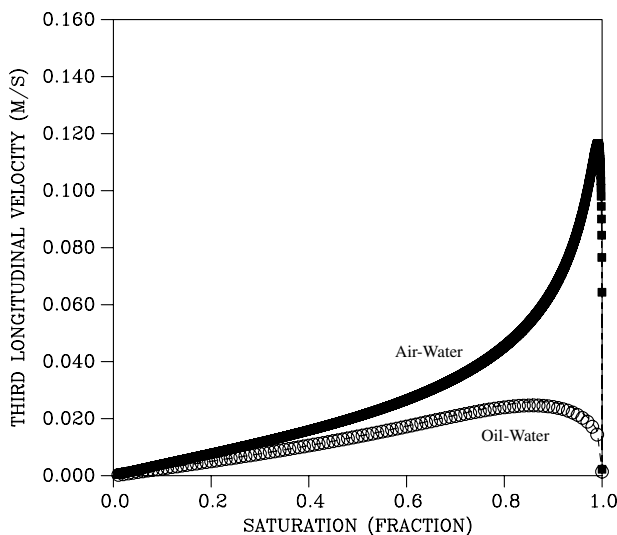


Figure 6. The velocities associated with the third mode of propagation $P3$, plotted as a function of water saturation. The values computed using the formulas of [Tuncay and Corapcioglu \(1996\)](#) are plotted as dashed (oil-water) and solid (air-water) lines.

also used in the analysis of the Massillon data conducted by [Tuncay and Corapcioglu \(1996\)](#). Because these curves have no analytic representation, we digitized the curves plotted in [Tuncay and Corapcioglu \(1996\)](#) and interpolated between the points using cubic splines. Thus, the relative permeabilities are approximate at the high and low saturation values where it is difficult to resolve the small

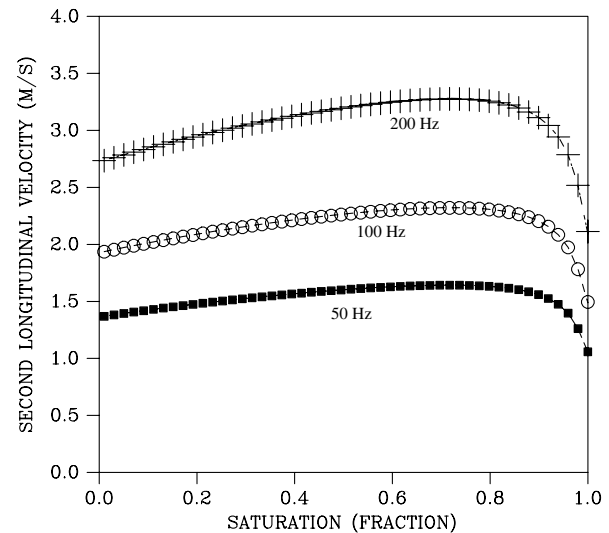


Figure 7. The velocities associated with the second or intermediate mode of propagation $P2$, plotted as a function of water saturation. The velocities are shown for three different frequencies: 50, 100, and 200 Hz. As in Figures 5 and 6, the values computed using methods in this paper are symbols; the values computed using the methods in [Tuncay and Corapcioglu \(1996\)](#) are solid and dashed lines.

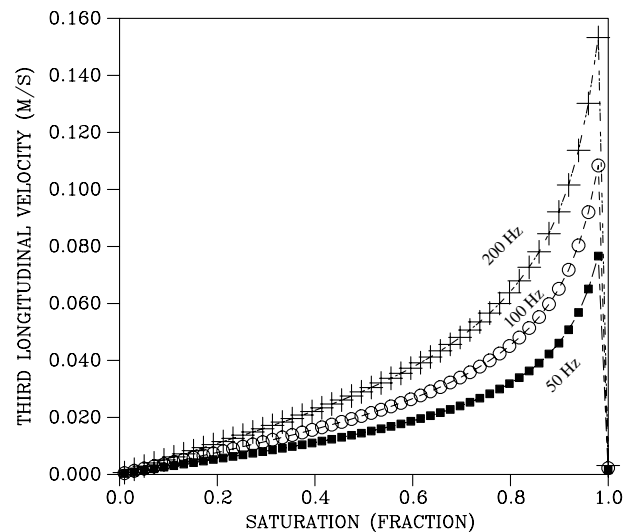


Figure 8. The velocities associated with the third mode of propagation $P3$, plotted as a function of water saturation. The velocities are shown for three different frequencies: 50, 100, and 200 Hz. The values computed using methods in this paper are symbols; the values computed using the methods in [Tuncay and Corapcioglu \(1996\)](#) are indicated by solid and dashed lines.

values. The capillary pressure function given above (see equation 73) was used in our modeling. These observations have been used in studies involving elastic wave propagation in a partially saturated porous medium (Tuncay and Corapcioglu, 1996; Berryman et al., 2002).

Using the parameters given above, the relative permeability curves plotted in Figure 9, and the capillary pressure function 73, we calculated the phase velocities for the longitudinal and transverse modes of propagation. Because of the diffusive nature of the second and third longitudinal modes, it is difficult to observe them experimentally. Thus, Murphy (1982) only has observations associated with the primary or first longitudinal mode and the transverse mode, as shown in Figure 10. We calculated the first longitudinal mode using cubic equation 36 with the parameters given above and the coefficients given in Appendix A and equations 37–40. The phase velocity associated with the transverse mode was estimated using equation 54. For comparison, we also computed the values using the formulas given in Tuncay and Corapcioglu (1996), plotted in Figure 10. Because of the difficulties in estimating the relative permeabilities and the sensitivity of the coefficients C_1 and C_2 at high and low saturations, we avoided making predictions of phase velocities for saturations near zero and one. Both techniques give sharp increases in longitudinal phase velocity for water saturations near one, but the exact values are fairly sensitive to how the relative permeabilities are calculated. Overall, there is good agreement between the observations of longitudinal and transverse phase velocity, the predictions by Tuncay and Corapcioglu (1996), and our predictions (Figure 10).

DISCUSSION

Following the approach of Tuncay (Tuncay, 1995; Tuncay and Corapcioglu, 1996, 1997) but using the formulation of Pride (1992, 1993), we have obtained governing equations for coupled deformation and two-phase flow. These equations are similar to corresponding expressions for coupled deformation and single-phase

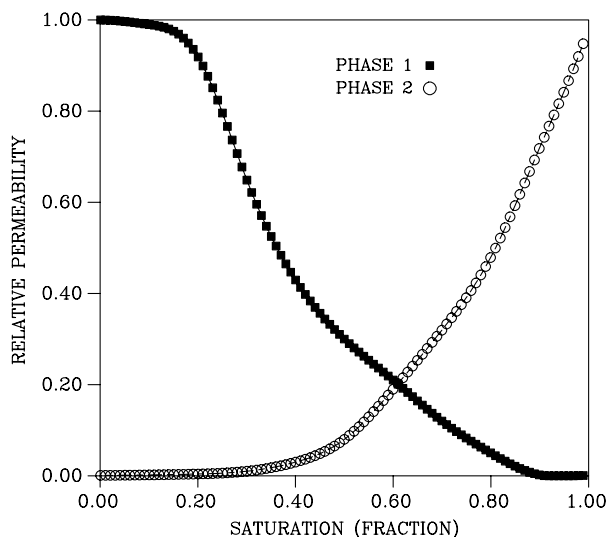


Figure 9. Relative permeability curves based upon the experiments of Wyckoff and Botset (1936) on the flow of gas-liquid mixtures through unconsolidated sands. The relative permeability functions are based upon cubic spline fits to a set of digitized points.

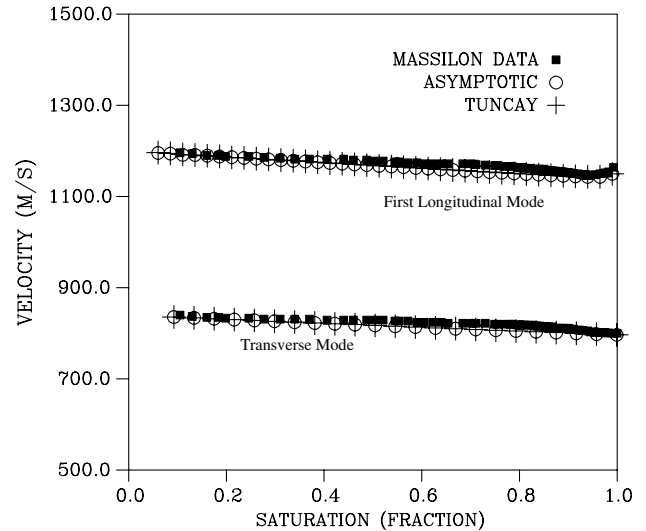


Figure 10. Observed (squares) and calculated (circles, crosses) phase velocities of the phase velocity of the transverse mode (lower curve) and the first longitudinal model (upper curve). The observed values were obtained from the experiments of Murphy (1982).

flow (Pride, 2005; Vasco, 2009). This similarity should aid in the interpretation of the coefficients and terms of the more complicated two-phase equations. Furthermore, the approach should make the extension to three phase conditions, such as oil, water, and gas, less difficult. Such an extension will result in a more complicated quartic equation for the longitudinal velocities. However, the solution of a quartic equation still has a closed-form expression in terms of its coefficients (Stahl, 1997, p. 124).

The equations given here unify several earlier investigations of two-phase flow in a deformable medium (Berryman et al., 1988; Santos et al., 1990; Tuncay and Corapcioglu, 1996, 1997; Lo et al., 2005) in which different assumptions were made regarding the inclusion of capillary pressure, the consideration of inertial effects of the fluid, and the presence or absence of heterogeneity in the medium. Here, as in Pride et al. (1992, 1993), we allow for the effects of capillary pressure as well as inertial effects due to the relative acceleration of the fluids with respect to the solid matrix. These effects are contained in the complex, integro-differential operator ν , whose form may vary, depending on the various forces included in the formulation. The methods presented in this paper are also applicable to more general models of fluid flow. For example, one could develop a model for wave propagation in a medium with patchy saturation (Dvorkin and Nur, 1998; Johnson, 2001). In addition, one could consider the mechanism of Biot flow and squirt flow, in which fluid movement into microcracks is accounted for (Dvorkin et al., 1994).

CONCLUSIONS

The asymptotic analysis presented in this paper leads to a semi-analytic solution for a medium with smoothly varying properties. Our preliminary analysis, restricted to zeroth-order terms, provides explicit expressions for the slowness of the longitudinal and transverse modes of propagation. As in a homogeneous medium, a cubic equation determines the slowness for the three modes of longitudinal propagation. The coefficients of the cubic equation are

expressed as sums of determinants of 3×3 matrices. The elements of the matrices are the coefficients in the governing equations. These determinant-based formulas for the coefficients are much simpler than previous explicit forms, are easy to implement in a computer program, and should reduce the occurrence of algebraic errors. Most importantly, the results are valid in the presence of smoothly varying heterogeneity. Thus, the explicit expressions for slowness provide a basis for traveltimes calculations and ray tracing in a heterogeneous poroelastic medium containing two fluid phases.

The asymptotic results pertaining to the phase velocity are the first steps toward a full solution of the coupled equations governing deformation and two-phase flow. Following earlier work on single-phase flow, it is straightforward, though rather laborious, to derive an expression for the amplitudes of the disturbances. Thus, one can derive the zeroth-order solution, obtained by considering the terms in the asymptotic power series corresponding to $n = 0$. The solution is valid for a medium with smoothly varying heterogeneity. However, the exact definition of smoothness is with respect to the scale length of the propagating disturbance. Thus, the notion of the medium smoothness does depend upon the frequency range of interest. If layering is present, it can be included as explicit boundaries within a given model, as can fault boundaries. The full expression for the zeroth-order asymptotic solution may be used for the efficient forward modeling of deformation and flow. Such modeling encompasses the hyperbolic, wavelike propagation of the elastic compressional and shear waves and the diffusive propagation that occurs primarily due to the presence of the fluid.

ACKNOWLEDGMENTS

This work was supported by the Assistant Secretary, Office of Basic Energy Sciences of the U. S. Department of Energy under contract DE-AC03-76SF00098. We would like to thank Jim Berryman, and by extension William Murphy, for supplying the data from the Massilon sandstone experiments.

APPENDIX A

THE CONSTITUTIVE EQUATIONS

In this appendix, we discuss the stress-strain relationships used in this paper. These equations have a long history and have evolved from the early constitutive equations for an elastic solid. First, the equations of elasticity were generalized to include a fluid (Kosten and Zwikker, 1941; Frenkel, 1944; Biot, 1956a, 1956b, 1962a, 1962b; Garg, 1971; Auriault, 1980; Pride et al., 1992). Then, two immiscible fluids were allowed to occupy the pore space (Bear et al., 1984; Garg and Nayfeh, 1986; Berryman et al., 1988; Santos et al., 1990; Tuncay and Corapcioglu, 1997; Lo et al., 2002, 2005). The stress-strain relationships depend on the elastic properties of the solid matrix and on the properties of the two fluids contained within the pore space. Specifically, the constitutive relationships depend upon the bulk modulus of the solid material comprising the grains of the matrix K_s and the bulk modulus of the solid skeleton as a whole, or the bulk modulus of the frame K_{fr} . In addition, the stress-strain relationship depends upon the shear modulus of the solid grains G_s and upon the shear modulus of the frame G_{fr} . The mechanical behavior of the poroelastic fluid-saturated body also depends upon the bulk moduli of the fluids, as denoted by

K_1 and K_2 . The behavior of the fluid-filled porous body is also a function of the pore fraction, as represented by the porosity ϕ and the fluid phase saturations S_1 and S_2 . The quantity α_i is the volume fraction of the fluid phase i and is related to the fluid saturation according to

$$\alpha_i = \phi S_i. \quad (\text{A-1})$$

Note that the fluid saturations sum to one, $S_1 + S_2 = 1$, because they fill the entire pore space. As is well known in the theory of the flow of immiscible fluids, in general there is a pressure differential between the two fluids occupying the pore space, the capillary pressure $P_{\text{cap}} = P_1 - P_2$ (Bear, 1972). This pressure differential, which is a function of the saturations, is responsible for the curvature of the interface between the pore fluids. Because the fluid saturations sum to unity, we can write the capillary pressure as a function of one of the fluid saturations — say, S_1 . Because we will be considering incremental pressures and saturations, changes with respect to some background average pressures and saturations, we can linearize the relationship between the incremental saturation change and the incremental pressure differences. Thus, we can write

$$P_1 - P_2 = \frac{dP_{\text{cap}}}{dS_1} \Delta S_1, \quad (\text{A-2})$$

assuming that one considers a small enough time increment such that the saturation change ΔS_1 is small.

The macroscopic stress-strain equations were derived by Tuncay and Corapcioglu (1997) using the method of averaging. This work generalizes the single-phase analysis of Pride et al. (1992). The coefficients in the equations are written in terms of the properties of the porous skeleton and the fluids:

$$N_1 = K_s(1 - \phi) - K_{fr}, \quad (\text{A-3})$$

$$N_2 = S_1 S_2 \frac{dP_{\text{cap}}}{dS_1}, \quad (\text{A-4})$$

$$N_3 = N_1 [K_1 S_1 N_2 + K_2 S_2 N_2 + K_1 K_2] + K_s^2 \phi [K_1 S_2 + K_2 S_1 + N_2]. \quad (\text{A-5})$$

In terms of these coefficients, the stress-strain relationship for the solid phase is given by

$$-(1 - \phi) \boldsymbol{\sigma}_s = [a_{11} \nabla \cdot \mathbf{u}_s + a_{12} \nabla \cdot \mathbf{u}_1 + a_{13} \nabla \cdot \mathbf{u}_2] \mathbf{I} + G_{fr} \left[\nabla \mathbf{u}_s + (\nabla \mathbf{u}_s)^T - \frac{2}{3} \nabla \cdot \mathbf{u}_s \mathbf{I} \right], \quad (\text{A-6})$$

where

$$a_{11} = \frac{K_s N_1 (1 - \phi) [K_1 N_2 S_1 + K_2 N_2 S_2 + K_1 K_2]}{N_3} + \frac{K_s^2 K_{fr} \phi [K_1 S_2 + K_2 S_1 + N_2]}{N_3}, \quad (\text{A-7})$$

$$a_{12} = \frac{K_1 K_s N_1 \phi S_1 (K_2 + N_2)}{N_3}, \quad (\text{A-8})$$

$$a_{13} = \frac{K_2 K_s N_1 \phi S_2 (K_1 + N_2)}{N_3}. \quad (\text{A-9})$$

Similarly, the full stress-strain relations for the two fluid components are

$$-\phi S_1 \boldsymbol{\sigma}_1 = [a_{21} \nabla \cdot \mathbf{u}_s + a_{22} \nabla \cdot \mathbf{u}_1 + a_{23} \nabla \cdot \mathbf{u}_2] \mathbf{I}, \quad (\text{A-10})$$

where

$$a_{21} = a_{12}, \quad (\text{A-11})$$

$$a_{22} = \frac{K_1 \phi S_1 [K_s^2 \phi K_2 S_1 + K_s^2 \phi N_2 + K_2 N_1 N_2 S_2]}{N_3}, \quad (\text{A-12})$$

$$a_{23} = \frac{K_1 K_2 S_2 \phi S_1 [K_s^2 \phi - N_1 N_2]}{N_3}, \quad (\text{A-13})$$

and

$$-\phi S_2 \boldsymbol{\sigma}_2 = [a_{31} \nabla \cdot \mathbf{u}_s + a_{32} \nabla \cdot \mathbf{u}_1 + a_{33} \nabla \cdot \mathbf{u}_2] \mathbf{I}, \quad (\text{A-14})$$

with

$$a_{31} = a_{13}, \quad (\text{A-15})$$

$$a_{32} = a_{23}, \quad (\text{A-16})$$

$$a_{33} = \frac{K_2 S_2 \phi [K_s^2 \phi K_1 S_2 + K_s^2 \phi N_2 + K_1 N_1 N_2 S_1]}{N_3}. \quad (\text{A-17})$$

We need the stress-strain relationships in terms of the solid displacements \mathbf{u}_s and the relative fluid displacements $\mathbf{w}_i = \mathbf{u}_i - \mathbf{u}_s$, the fluid displacement relative to the current position of the solid matrix. Thus, we add and subtract appropriately weighted \mathbf{u}_s terms. For example, equation A-6 can be written

$$\begin{aligned} -(1 - \phi) \boldsymbol{\sigma}_s &= [a_{1s} \nabla \cdot \mathbf{u}_s + a_{12} \nabla \cdot \mathbf{w}_1 + a_{13} \nabla \cdot \mathbf{w}_2] \mathbf{I} \\ &+ G_{fr} \left[\nabla \mathbf{u}_s + (\nabla \mathbf{u}_s)^T - \frac{2}{3} \nabla \cdot \mathbf{u}_s \mathbf{I} \right], \end{aligned} \quad (\text{A-18})$$

where

$$a_{1s} = a_{11} + a_{12} + a_{13}. \quad (\text{A-19})$$

Similarly for the two fluid phases, we can write

$$-\phi S_1 \boldsymbol{\sigma}_1 = [a_{2s} \nabla \cdot \mathbf{u}_s + a_{22} \nabla \cdot \mathbf{w}_1 + a_{23} \nabla \cdot \mathbf{w}_2] \mathbf{I} \quad (\text{A-20})$$

and

$$-\phi S_2 \boldsymbol{\sigma}_2 = [a_{3s} \nabla \cdot \mathbf{u}_s + a_{32} \nabla \cdot \mathbf{w}_1 + a_{33} \nabla \cdot \mathbf{w}_2] \mathbf{I}, \quad (\text{A-21})$$

where

$$a_{2s} = a_{21} + a_{22} + a_{23} \quad (\text{A-22})$$

and

$$a_{3s} = a_{31} + a_{32} + a_{33}. \quad (\text{A-23})$$

We rename the coefficients in the stress-strain relationships given above to bring them closer to the form of the stress-strain relationships for a single fluid phase in a poroelastic medium (Pride, 2005):

$$\begin{aligned} -(1 - \phi) \boldsymbol{\sigma}_s &= [K_u \nabla \cdot \mathbf{u}_s + C_{s1} \nabla \cdot \mathbf{w}_1 + C_{s2} \nabla \cdot \mathbf{w}_2] \mathbf{I} \\ &+ G_m \left[\nabla \mathbf{u}_s + (\nabla \mathbf{u}_s)^T - \frac{2}{3} \nabla \cdot \mathbf{u}_s \mathbf{I} \right], \end{aligned} \quad (\text{A-24})$$

$$-\phi S_1 \boldsymbol{\sigma}_1 = [C_{1s} \nabla \cdot \mathbf{u}_s + M_{11} \nabla \cdot \mathbf{w}_1 + M_{12} \nabla \cdot \mathbf{w}_2] \mathbf{I}, \quad (\text{A-25})$$

and

$$-\phi S_2 \boldsymbol{\sigma}_2 = [C_{2s} \nabla \cdot \mathbf{u}_s + M_{21} \nabla \cdot \mathbf{w}_1 + M_{22} \nabla \cdot \mathbf{w}_2] \mathbf{I}, \quad (\text{A-26})$$

where the coefficients are given by G_{fr} and the parameters a_{ij} :

$$K_u = a_{1s}, \quad (\text{A-27})$$

$$C_{s1} = a_{12}, \quad (\text{A-28})$$

$$C_{s2} = a_{13}, \quad (\text{A-29})$$

$$G_m = G_{fr}, \quad (\text{A-30})$$

$$C_{1s} = a_{2s}, \quad (\text{A-31})$$

$$M_{11} = a_{22}, \quad (\text{A-32})$$

$$M_{12} = a_{23}, \quad (\text{A-33})$$

$$C_{2s} = a_{3s}, \quad (\text{A-34})$$

$$M_{21} = a_{32}, \quad (\text{A-35})$$

$$M_{22} = a_{33}. \quad (\text{A-36})$$

APPENDIX B

APPLICATION OF THE METHOD OF MULTIPLE SCALES TO EQUATIONS GOVERNING COUPLED DEFORMATION AND TWO-PHASE FLOW

In this appendix, we use the method of multiple scales to obtain a system of equations constraining the zeroth-order amplitudes of the

solid displacement \mathbf{U}_s^0 and the fluid velocities \mathbf{W}_1^0 and \mathbf{W}_2^0 in a heterogeneous poroelastic medium saturated by two fluids. The condition that these equations have a nontrivial solution is sufficient to provide equations for the phase velocities of the various modes of propagation. The motivation for the method of multiple scales is presented in the main body of the text. In particular, see the discussion surrounding equations 25–30.

Let us begin with the first of the governing equations 19, after expanding all of the spatial derivatives:

$$\begin{aligned} \nabla G_m \cdot \nabla \mathbf{U}_s + \nabla G_m \cdot (\nabla \mathbf{U}_s)^T - \frac{2}{3} \nabla G_m \cdot [(\nabla \cdot \mathbf{U}_s) \mathbf{I}] \\ + G_m \nabla \cdot \nabla \mathbf{U}_s + G_m \nabla \cdot (\nabla \mathbf{U}_s)^T - \frac{2}{3} G_m \nabla \cdot [(\nabla \cdot \mathbf{U}_s) \mathbf{I}] \\ + \nabla K_u \nabla \cdot \mathbf{U}_s + K_u \nabla (\nabla \cdot \mathbf{U}_s) + \nabla C_{s1} \nabla \cdot \mathbf{W}_1 \\ + C_{s1} \nabla (\nabla \cdot \mathbf{W}_1) + \nabla C_{s2} \nabla \cdot \mathbf{W}_2 + C_{s2} \nabla (\nabla \cdot \mathbf{W}_2) \\ + \nu_s \mathbf{U}_s + \xi_1 \mathbf{W}_1 + \xi_2 \mathbf{W}_2 = 0. \end{aligned} \quad (\text{B-1})$$

The first step involves reformulating the governing equations in terms of the slow variables, introduced in equation 25. To do this, we rewrite the differential operators in slow coordinates, as in equation 29. We then substitute the series representations for the vectors \mathbf{U}_s and \mathbf{W}_i (see equations 26 and 27), retaining only those terms containing $\epsilon^0 \sim 1$ and ϵ^1 . We use the definition of $\mathbf{I} = \nabla \theta$ to arrive at

$$\begin{aligned} \epsilon \nabla G_m \cdot \left(\mathbf{I} \frac{\partial \mathbf{U}_s}{\partial \theta} \right) + \epsilon \nabla G_m \cdot \left(\mathbf{I} \frac{\partial \mathbf{U}_s}{\partial \theta} \right)^T - \epsilon \frac{2}{3} \nabla G_m \cdot \left[\left(\mathbf{I} \cdot \frac{\partial \mathbf{U}_s}{\partial \theta} \right) \mathbf{I} \right] \\ + \epsilon G_m \nabla \cdot \left(\mathbf{I} \frac{\partial \mathbf{U}_s}{\partial \theta} \right) + \epsilon G_m \mathbf{I} \cdot \nabla \left(\frac{\partial \mathbf{U}_s}{\partial \theta} \right) + G_m \mathbf{I} \cdot \left(\mathbf{I} \frac{\partial^2 \mathbf{U}_s}{\partial \theta^2} \right) \\ + \epsilon G_m \nabla \cdot \left(\mathbf{I} \frac{\partial \mathbf{U}_s}{\partial \theta} \right)^T + \epsilon G_m \mathbf{I} \cdot \nabla \left(\frac{\partial \mathbf{U}_s}{\partial \theta} \right)^T + G_m \mathbf{I} \cdot \left(\mathbf{I} \frac{\partial^2 \mathbf{U}_s}{\partial \theta^2} \right)^T \\ - \epsilon \frac{2}{3} G_m \nabla \cdot \left(\mathbf{I} \cdot \frac{\partial \mathbf{U}_s}{\partial \theta} \right) \mathbf{I} - \epsilon \frac{2}{3} G_m \mathbf{I} \cdot \left(\nabla \cdot \frac{\partial \mathbf{U}_s}{\partial \theta} \right) \mathbf{I} \\ - \frac{2}{3} G_m \mathbf{I} \cdot \left(\mathbf{I} \cdot \frac{\partial^2 \mathbf{U}_s}{\partial \theta^2} \right) \mathbf{I} + \epsilon \nabla K_u \left(\mathbf{I} \cdot \frac{\partial \mathbf{U}_s}{\partial \theta} \right) + \epsilon K_u \nabla \left(\mathbf{I} \cdot \frac{\partial \mathbf{U}_s}{\partial \theta} \right) \\ + \epsilon K_u \mathbf{I} \left(\nabla \cdot \frac{\partial \mathbf{U}_s}{\partial \theta} \right) + K_u \mathbf{I} \left(\mathbf{I} \cdot \frac{\partial^2 \mathbf{U}_s}{\partial \theta^2} \right) + \epsilon \nabla C_{s1} \left(\mathbf{I} \cdot \frac{\partial \mathbf{W}_1}{\partial \theta} \right) \\ + \epsilon C_{s1} \nabla \left(\mathbf{I} \cdot \frac{\partial \mathbf{W}_1}{\partial \theta} \right) + \epsilon C_{s1} \mathbf{I} \left(\nabla \cdot \frac{\partial \mathbf{W}_1}{\partial \theta} \right) + C_{s1} \mathbf{I} \left(\mathbf{I} \cdot \frac{\partial^2 \mathbf{W}_1}{\partial \theta^2} \right) \\ + \epsilon \nabla C_{s2} \left(\mathbf{I} \cdot \frac{\partial \mathbf{W}_2}{\partial \theta} \right) + \epsilon C_{s2} \nabla \left(\mathbf{I} \cdot \frac{\partial \mathbf{W}_2}{\partial \theta} \right) + \epsilon C_{s2} \mathbf{I} \left(\nabla \cdot \frac{\partial \mathbf{W}_2}{\partial \theta} \right) \\ + C_{s2} \mathbf{I} \left(\mathbf{I} \cdot \frac{\partial^2 \mathbf{W}_2}{\partial \theta^2} \right) + \nu_s \mathbf{U}_s + \xi_1 \mathbf{W}_1 + \xi_2 \mathbf{W}_2 = 0. \end{aligned} \quad (\text{B-2})$$

We can write equation B-2 more compactly if we use the fact that

$$\frac{\partial \mathbf{U}_s}{\partial \theta} = i \mathbf{U}_s \quad (\text{B-3})$$

and

$$\frac{\partial \mathbf{W}_i}{\partial \theta} = i \mathbf{W}_i, \quad (\text{B-4})$$

which follows from the form of solutions 26 and 27. Making these substitutions, we can rewrite equation B-2 as

$$\begin{aligned} \epsilon \nabla G_m \cdot (i \mathbf{U}_s) + \epsilon \nabla G_m \cdot (i \mathbf{U}_s)^T - \epsilon \frac{2}{3} \nabla G_m \cdot [(i \mathbf{I} \cdot \mathbf{U}_s) \mathbf{I}] \\ + \epsilon G_m \nabla \cdot (i \mathbf{U}_s) + \epsilon G_m \mathbf{I} \cdot \nabla (i \mathbf{U}_s) - G_m \mathbf{I} \cdot (i \mathbf{U}_s) \\ + \epsilon G_m \nabla \cdot (i \mathbf{U}_s)^T + \epsilon G_m \mathbf{I} \cdot (\nabla i \mathbf{U}_s)^T - G_m \mathbf{I} \cdot (i \mathbf{U}_s)^T \\ - \epsilon \frac{2}{3} G_m \nabla \cdot (i \mathbf{I} \cdot \mathbf{U}_s) \mathbf{I} - \epsilon \frac{2}{3} G_m \mathbf{I} \cdot (\nabla \cdot i \mathbf{U}_s) \mathbf{I} \\ + \frac{2}{3} G_m \mathbf{I} \cdot (\mathbf{I} \cdot \mathbf{U}_s) \mathbf{I} + \epsilon \nabla K_u (i \mathbf{I} \cdot \mathbf{U}_s) + \epsilon K_u \nabla (i \mathbf{I} \cdot \mathbf{U}_s) \\ + \epsilon K_u \mathbf{I} (\nabla \cdot i \mathbf{U}_s) - K_u \mathbf{I} (\mathbf{I} \cdot \mathbf{U}_s) + \epsilon \nabla C_{s1} (i \mathbf{I} \cdot \mathbf{W}_1) \\ + \epsilon C_{s1} \nabla (i \mathbf{I} \cdot \mathbf{W}_1) + \epsilon C_{s1} \mathbf{I} (\nabla \cdot i \mathbf{W}_1) - C_{s1} \mathbf{I} (\mathbf{I} \cdot \mathbf{W}_1) \\ + \epsilon \nabla C_{s2} (i \mathbf{I} \cdot \mathbf{W}_2) + \epsilon C_{s2} \nabla (i \mathbf{I} \cdot \mathbf{W}_2) + \epsilon C_{s2} \mathbf{I} (\nabla \cdot i \mathbf{W}_2) \\ - C_{s2} \mathbf{I} (\mathbf{I} \cdot \mathbf{W}_2) + \nu_s \mathbf{U}_s + \xi_1 \mathbf{W}_1 + \xi_2 \mathbf{W}_2 = 0. \end{aligned} \quad (\text{B-5})$$

From equation B-5, we can obtain all of the terms necessary for the first of the three governing equations 19. In particular, we can extract all terms of order $\epsilon^0 \sim 1$ that are required to determine an expression for phase.

We also need the zeroth-order terms for the two fluid equations 20 and 21. We use index notation to represent the pair of equations by a single expression. The expanded version of the index equation is given by

$$\begin{aligned} \nabla C_{is} \nabla \cdot \mathbf{U}_s + C_{is} \nabla \nabla \cdot \mathbf{U}_s + \nabla M_{i1} \nabla \cdot \mathbf{W}_1 \\ + M_{i1} \nabla \nabla \cdot \mathbf{W}_1 + \nabla M_{i2} \nabla \cdot \mathbf{W}_2 \\ + M_{i2} \nabla \nabla \cdot \mathbf{W}_2 + \nu_i \mathbf{U}_s + \Gamma_i \mathbf{W}_i = 0, \end{aligned} \quad (\text{B-6})$$

where the index i signifies the fluid that is under consideration. Substituting the differential operators and retaining terms of order ϵ^0 and ϵ^1 , and using the definition of $\nabla \theta = \mathbf{I}$,

$$\begin{aligned} \epsilon \nabla C_{is} \left(\mathbf{I} \cdot \frac{\partial \mathbf{U}_s}{\partial \theta} \right) + \epsilon C_{is} \nabla \left(\mathbf{I} \cdot \frac{\partial \mathbf{U}_s}{\partial \theta} \right) + \epsilon C_{is} \mathbf{I} \left(\nabla \cdot \frac{\partial \mathbf{U}_s}{\partial \theta} \right) \\ + C_{is} \mathbf{I} \left(\mathbf{I} \cdot \frac{\partial^2 \mathbf{U}_s}{\partial \theta^2} \right) + \epsilon \nabla M_{i1} \left(\mathbf{I} \cdot \frac{\partial \mathbf{W}_1}{\partial \theta} \right) \\ + \epsilon M_{i1} \nabla \left(\mathbf{I} \cdot \frac{\partial \mathbf{W}_1}{\partial \theta} \right) + \epsilon M_{i1} \mathbf{I} \left(\nabla \cdot \frac{\partial \mathbf{W}_1}{\partial \theta} \right) \\ + M_{i1} \mathbf{I} \left(\mathbf{I} \cdot \frac{\partial^2 \mathbf{W}_1}{\partial \theta^2} \right) + \epsilon \nabla M_{i2} \left(\mathbf{I} \cdot \frac{\partial \mathbf{W}_2}{\partial \theta} \right) \\ + \epsilon M_{i2} \nabla \left(\mathbf{I} \cdot \frac{\partial \mathbf{W}_2}{\partial \theta} \right) + \epsilon M_{i2} \mathbf{I} \left(\nabla \cdot \frac{\partial \mathbf{W}_2}{\partial \theta} \right) \\ + M_{i2} \mathbf{I} \left(\mathbf{I} \cdot \frac{\partial^2 \mathbf{W}_2}{\partial \theta^2} \right) + \nu_i \mathbf{U}_s + \Gamma_i \mathbf{W}_i = 0. \end{aligned} \quad (\text{B-7})$$

Using the property of the partial derivatives given by equations B-3 and B-4, we can write equation B-7 as

$$\begin{aligned}
 & i\varepsilon \nabla C_{is}(\mathbf{I} \cdot \mathbf{U}_s) + i\varepsilon C_{is}[\nabla(\mathbf{I} \cdot \mathbf{U}_s) + \mathbf{I}(\nabla \cdot \mathbf{U}_s)] \\
 & - C_{is}\mathbf{I}(\mathbf{I} \cdot \mathbf{U}_s) + i\varepsilon \nabla M_{i1}(\mathbf{I} \cdot \mathbf{W}_1) + i\varepsilon M_{i1}[\nabla(\mathbf{I} \cdot \mathbf{W}_1) \\
 & + \mathbf{I}(\nabla \cdot \mathbf{W}_1)] - M_{i1}\mathbf{I}(\mathbf{I} \cdot \mathbf{W}_1) + i\varepsilon \nabla M_{i2}(\mathbf{I} \cdot \mathbf{W}_2) \\
 & + i\varepsilon M_{i2}[\nabla(\mathbf{I} \cdot \mathbf{W}_2) + \mathbf{I}(\nabla \cdot \mathbf{W}_2)] \\
 & - M_{i2}\mathbf{I}(\mathbf{I} \cdot \mathbf{W}_2) + \nu_i \mathbf{U}_s + \Gamma_i \mathbf{W}_i = 0
 \end{aligned} \tag{B-8}$$

for $i = 1, 2$ for the two fluids, respectively.

Terms of order zero

In this subsection, we consider terms of the lowest order in ε , terms of order zero. For smoothly varying heterogeneity, such terms are the most significant. Gathering terms of zeroth-order from equation B-5 leads to

$$\begin{aligned}
 & -G_m l^2 \mathbf{U}_s^0 - G_m \mathbf{II} \cdot \mathbf{U}_s^0 + \frac{2}{3} G_m \mathbf{II} \cdot \mathbf{U}_s^0 - K_u \mathbf{II} \cdot \mathbf{U}_s^0 + \nu_s \mathbf{U}_s^0 \\
 & - C_{s1} \mathbf{II} \cdot \mathbf{W}_1^0 - C_{s2} \mathbf{II} \cdot \mathbf{W}_2^0 + \xi_1 \mathbf{W}_1^0 + \xi_2 \mathbf{W}_2^0 = 0,
 \end{aligned} \tag{B-9}$$

where

$$\mathbf{II} \cdot \mathbf{U}_s^0 = \mathbf{I}(\mathbf{I} \cdot \mathbf{U}_s^0). \tag{B-10}$$

Note that we can represent equation B-10 as an operator, a dyadic (Ben-Menahem and Singh, 1981; Chapman, 2004) applied to \mathbf{U}_s^0 :

$$\mathbf{I}(\mathbf{I} \cdot \mathbf{U}_s^0) = \mathbf{I}(\mathbf{I} \cdot \mathbf{I})\mathbf{U}_s^0, \tag{B-11}$$

where \mathbf{I} is the identity matrix with ones on the diagonal and zeros off the diagonal. Alternatively, one may think of the dyadic \mathbf{II} as the vector outer product \mathbf{II}^T , where \mathbf{I}^T signifies the transpose of \mathbf{I} , converting the column vector \mathbf{I} to the row vector \mathbf{I}^T .

Combining like terms and defining the coefficients

$$\alpha = \nu_s - G_m l^2 \tag{B-12}$$

and

$$\beta = K_u + \frac{1}{3} G_m, \tag{B-13}$$

we can rewrite equation B-9 as

$$\begin{aligned}
 & \alpha \mathbf{U}_s^0 - \beta \mathbf{II} \cdot \mathbf{U}_s^0 + \xi_1 \mathbf{W}_1^0 - C_{s1} \mathbf{II} \cdot \mathbf{W}_1^0 + \xi_2 \mathbf{W}_2^0 \\
 & - C_{s2} \mathbf{II} \cdot \mathbf{W}_2^0 = 0.
 \end{aligned} \tag{B-14}$$

We can treat the equations pertaining to the two fluids, as expressed in B-6, similarly. Collecting the zeroth-order terms in equation B-8 produces

$$\nu_i \mathbf{U}_s^0 - C_{is} \mathbf{II} \cdot \mathbf{U}_s^0 - M_{i1} \mathbf{II} \cdot \mathbf{W}_1^0 - M_{i2} \mathbf{II} \cdot \mathbf{W}_2^0 + \Gamma_i \mathbf{W}_i^0 = 0, \tag{B-15}$$

where the index i takes the values one or two, depending on the fluid under consideration.

APPENDIX C

REDUCTION OF THE DETERMINANT

In this appendix, we demonstrate that the vanishing of the determinant of the 9×9 coefficient matrix in equation 31,

$$\mathbf{\Gamma} = \begin{pmatrix} \alpha \mathbf{I} - \beta \mathbf{II} \cdot \mathbf{I} & \xi_1 \mathbf{I} - C_{s1} \mathbf{II} \cdot \mathbf{I} & \xi_2 \mathbf{I} - C_{s2} \mathbf{II} \cdot \mathbf{I} \\ \nu_1 \mathbf{I} - C_{1s} \mathbf{II} \cdot \mathbf{I} & \Gamma_1 \mathbf{I} - M_{11} \mathbf{II} \cdot \mathbf{I} & -M_{12} \mathbf{II} \cdot \mathbf{I} \\ \nu_2 \mathbf{I} - C_{2s} \mathbf{II} \cdot \mathbf{I} & -M_{21} \mathbf{II} \cdot \mathbf{I} & \Gamma_2 \mathbf{I} - M_{22} \mathbf{II} \cdot \mathbf{I} \end{pmatrix}, \tag{C-1}$$

is equivalent to the vanishing of the determinant of a much smaller 3×3 matrix. The determinant of a matrix is given by the product of its eigenvalues (Noble and Daniel, 1977). Thus, the vanishing of the determinant is equivalent to the vanishing of one or more eigenvalues of the matrix $\mathbf{\Gamma}$. Furthermore, there will be an eigenvector associated with the zero eigenvalue.

Based upon physical considerations, in particular the polarizations of the modes of propagation in a poroelastic medium and the structure of the matrix C-1, the vectors

$$\mathbf{e}^l = \begin{pmatrix} y_1 \mathbf{I} \\ y_2 \mathbf{I} \\ y_3 \mathbf{I} \end{pmatrix}, \tag{C-2}$$

$$\mathbf{e}_1^\perp = \begin{pmatrix} z_1 \mathbf{I}_1^\perp \\ z_2 \mathbf{I}_1^\perp \\ z_3 \mathbf{I}_1^\perp \end{pmatrix}, \tag{C-3}$$

and

$$\mathbf{e}_2^\perp = \begin{pmatrix} t_1 \mathbf{I}_2^\perp \\ t_2 \mathbf{I}_2^\perp \\ t_3 \mathbf{I}_2^\perp \end{pmatrix} \tag{C-4}$$

are suggested as potential eigenvectors of the matrix $\mathbf{\Gamma}$. Here, \mathbf{I}_1^\perp and \mathbf{I}_2^\perp are two orthogonal vectors lying in the plane perpendicular to \mathbf{I} . Physically, the vector \mathbf{e}^l corresponds to longitudinal propagation when the fluid and solid displacements are parallel to the direction of propagation. Conversely, the vectors \mathbf{e}_1^\perp and \mathbf{e}_2^\perp correspond to transverse motion in which the direction of fluid and solid displacement is perpendicular to the direction of propagation. The physical motivation is from wave propagation in a homogeneous medium. In a homogeneous medium, one can use potentials to decompose an elastic disturbance into a longitudinal mode of propagation and two transverse modes of propagation (Aki and Richards, 1980). The structure of the matrix $\mathbf{\Gamma}$ also suggests that the vectors C-2, C-3, and C-4 are potential eigenvectors. Specifically, each 3×3 submatrix in $\mathbf{\Gamma}$ contains the terms \mathbf{I} and $\mathbf{II} \cdot \mathbf{I}$. When these terms are multiplied by \mathbf{I} , the results are proportional to \mathbf{I} . When the terms are multiplied by \mathbf{I}_1^\perp and \mathbf{I}_2^\perp , the first term gives the same vector but the second term vanishes. Thus, the vector \mathbf{I} , and vectors perpendicular to it provide special directions for the matrix $\mathbf{\Gamma}$.

For illustration, we consider the eigenvector \mathbf{e}^l associated with the longitudinal modes of propagation, displacement in the direction of propagation \mathbf{I} . Because it is an eigenvector, the vector \mathbf{e}^l satisfies the equation

$$\mathbf{\Gamma} \mathbf{e}^l = \lambda \mathbf{e}^l. \quad (\text{C-5})$$

Furthermore, because we are interested in the case in which the determinant vanishes, the eigenvalue of interest is the one that vanishes, reducing equation C-5 to

$$\mathbf{\Gamma} \mathbf{e}^l = 0. \quad (\text{C-6})$$

From the algebraic form of the coefficient matrix $\mathbf{\Gamma}$ and the form of the eigenvector \mathbf{e}^l , equation C-6 is equivalent to

$$\begin{pmatrix} [\alpha - \beta l^2] \mathbf{I} & [\xi_1 - C_{s1} l^2] \mathbf{I} & [\xi_2 - C_{s2} l^2] \mathbf{I} \\ [\nu_1 - C_{1s} l^2] \mathbf{I} & [\Gamma_1 - M_{11} l^2] \mathbf{I} & -M_{12} l^2 \mathbf{I} \\ [\nu_2 - C_{2s} l^2] \mathbf{I} & -M_{21} l^2 \mathbf{I} & [\Gamma_2 - M_{22} l^2] \mathbf{I} \end{pmatrix} \times \begin{pmatrix} y_1 \mathbf{I} \\ y_2 \mathbf{I} \\ y_3 \mathbf{I} \end{pmatrix} = 0. \quad (\text{C-7})$$

The requirement that this equation have a nontrivial solution is the vanishing of the determinant of the coefficient matrix,

$$\det \begin{pmatrix} [\alpha - \beta l^2] \mathbf{I} & [\xi_1 - C_{s1} l^2] \mathbf{I} & [\xi_2 - C_{s2} l^2] \mathbf{I} \\ [\nu_1 - C_{1s} l^2] \mathbf{I} & [\Gamma_1 - M_{11} l^2] \mathbf{I} & -M_{12} l^2 \mathbf{I} \\ [\nu_2 - C_{2s} l^2] \mathbf{I} & -M_{21} l^2 \mathbf{I} & [\Gamma_2 - M_{22} l^2] \mathbf{I} \end{pmatrix} = 0. \quad (\text{C-8})$$

At this point, we invoke a theorem from linear algebra regarding the determinant of a matrix composed of block submatrices (Silvester, 2000). The theorem states that the determinant of a matrix tensor product

$$\mathbf{L} \otimes \mathbf{Q} = \begin{pmatrix} l_{11} \mathbf{Q} & l_{12} \mathbf{Q} & l_{13} \mathbf{Q} \\ l_{21} \mathbf{Q} & l_{22} \mathbf{Q} & l_{23} \mathbf{Q} \\ l_{31} \mathbf{Q} & l_{32} \mathbf{Q} & l_{33} \mathbf{Q} \end{pmatrix}, \quad (\text{C-9})$$

where \mathbf{Q} is a 3×3 matrix and

$$\mathbf{L} = \begin{pmatrix} l_{11} & l_{12} & l_{13} \\ l_{21} & l_{22} & l_{23} \\ l_{31} & l_{32} & l_{33} \end{pmatrix}, \quad (\text{C-10})$$

is given by

$$\det(\mathbf{L} \otimes \mathbf{Q}) = (\det \mathbf{L})(\det \mathbf{Q})^3. \quad (\text{C-11})$$

Applying this theorem to the coefficient matrix in equation C-8 and making use of the fact that \mathbf{Q} is the identity matrix, we derive the condition

$$\det \begin{pmatrix} \alpha - \beta l^2 & \xi_1 - C_{s1} l^2 & \xi_2 - C_{s2} l^2 \\ \nu_1 - C_{1s} l^2 & \Gamma_1 - M_{11} l^2 & -M_{12} l^2 \\ \nu_2 - C_{2s} l^2 & -M_{21} l^2 & \Gamma_2 - M_{22} l^2 \end{pmatrix} = 0, \quad (\text{C-12})$$

the vanishing of the determinant of a 3×3 matrix.

APPENDIX D

COMPUTING THE DETERMINANT FOR THE LONGITUDINAL MODE OF PROPAGATION

In this appendix, we detail the computation of the determinant of the matrix

$$\mathbf{M} = \begin{pmatrix} \nu_s - Hs & \xi_1 - C_{s1}s & \xi_2 - C_{s2}s \\ \nu_1 - C_{1s}s & \Gamma_1 - M_{11}s & -M_{12}s \\ \nu_2 - C_{2s}s & -M_{21}s & \Gamma_2 - M_{22}s \end{pmatrix}, \quad (\text{D-1})$$

where $s = l^2$. The principle that we apply repeatedly relates to the determinant of a matrix containing a column in which each element is the sum of two terms. A theorem in linear algebra shows that the determinant of such a matrix can be written as the sum of two determinants, each of which contains one element of the sum (Noble and Daniel, 1977, p. 200). We illustrate this principle by an application to the matrix \mathbf{M} given above. Each element of the first column of this matrix is the sum of two terms. Thus, we can write the determinant of \mathbf{M} as

$$\begin{aligned} \det \begin{pmatrix} \nu_s - Hs & \xi_1 - C_{s1}s & \xi_2 - C_{s2}s \\ \nu_1 - C_{1s}s & \Gamma_1 - M_{11}s & -M_{12}s \\ \nu_2 - C_{2s}s & -M_{21}s & \Gamma_2 - M_{22}s \end{pmatrix} \\ = \det \begin{pmatrix} \nu_s & \xi_1 - C_{s1}s & \xi_2 - C_{s2}s \\ \nu_1 & \Gamma_1 - M_{11}s & -M_{12}s \\ \nu_2 & -M_{21}s & \Gamma_2 - M_{22}s \end{pmatrix} \\ - s \det \begin{pmatrix} H & \xi_1 - C_{s1}s & \xi_2 - C_{s2}s \\ C_{1s} & \Gamma_1 - M_{11}s & -M_{12}s \\ C_{2s} & -M_{21}s & \Gamma_2 - M_{22}s \end{pmatrix}. \end{aligned} \quad (\text{D-2})$$

We can apply this principle recursively, first to the second column of each of the component matrices in equation D-2 and then to the third column of each of the component determinants, obtaining a cubic equation in s . We can write the cubic equation compactly as

$$Q_3 s^3 + Q_2 s^2 + Q_1 s + Q_0 = 0 \quad (\text{D-3})$$

if we define the coefficients

$$Q_3 = \det \begin{pmatrix} H & C_{s1} & C_{s2} \\ C_{1s} & M_{11} & M_{12} \\ C_{2s} & M_{21} & M_{22} \end{pmatrix}, \quad (\text{D-4})$$

$$\begin{aligned} Q_2 = & -\det \begin{pmatrix} \nu_s & C_{s1} & C_{s2} \\ \nu_1 & M_{11} & M_{12} \\ \nu_2 & M_{21} & M_{22} \end{pmatrix} - \det \begin{pmatrix} H & \xi_1 & C_{s2} \\ C_{1s} & \Gamma_1 & M_{12} \\ C_{2s} & 0 & M_{22} \end{pmatrix} \\ & - \det \begin{pmatrix} H & C_{s1} & \xi_2 \\ C_{1s} & M_{11} & 0 \\ C_{2s} & M_{21} & \Gamma_2 \end{pmatrix}, \end{aligned} \quad (\text{D-5})$$

$$Q_1 = \det \begin{pmatrix} \nu_s & \xi_1 & C_{s2} \\ \nu_1 & \Gamma_1 & M_{12} \\ \nu_2 & 0 & M_{22} \end{pmatrix} + \det \begin{pmatrix} \nu_s & C_{s1} & \xi_2 \\ \nu_1 & M_{11} & 0 \\ \nu_2 & M_{21} & \Gamma_2 \end{pmatrix} \\ + \det \begin{pmatrix} H & \xi_1 & \xi_2 \\ C_{1s} & \Gamma_1 & 0 \\ C_{2s} & 0 & \Gamma_2 \end{pmatrix}, \quad (\text{D-6})$$

$$Q_0 = -\det \begin{pmatrix} \nu_s & \xi_1 & \xi_2 \\ \nu_1 & \Gamma_1 & 0 \\ \nu_2 & 0 & \Gamma_2 \end{pmatrix}. \quad (\text{D-7})$$

REFERENCES

- Aki, K., and P. G. Richards, 1980, Quantitative seismology: W. H. Freeman & Co.
- Anile, A. M., J. K. Hunter, P. Pantano, and G. Russo, 1993, Ray methods for nonlinear waves in fluids and plasmas: Longman Scientific and Technical.
- Auriault, J. L., 1980, Dynamic behavior of a porous medium saturated by a Newtonian fluid: International Journal of Engineering Science, **18**, no. 6, 775–785, doi: [10.1016/0020-7225\(80\)90025-7](https://doi.org/10.1016/0020-7225(80)90025-7).
- Bear, J., 1972, Dynamics of fluids in porous media: Elsevier.
- Bear, J., M. Y. Corapcioglu, and J. Balakrishna, 1984, Modeling of centrifugal filtration in unsaturated deformable porous media: Advances in Water Resources, **7**, no. 4, 150–167, doi: [10.1016/0309-1708\(84\)90013-7](https://doi.org/10.1016/0309-1708(84)90013-7).
- Ben-Menahem, A., and S. J. Singh, 1981, Seismic waves and sources: Springer Verlag.
- Berryman, J. G., P. A. Berge, and B. P. Bonner, 2002, Estimating rock porosity and fluid saturation using only seismic velocities: Geophysics, **67**, 391–404, doi: [10.1190/1.1468599](https://doi.org/10.1190/1.1468599).
- Berryman, J. G., L. Thigpen, and R. C. Y. Chin, 1988, Bulk elastic wave propagation in partially saturated porous solids: Journal of the Acoustical Society of America, **84**, 360–373, doi: [10.1121/1.396938](https://doi.org/10.1121/1.396938).
- Biot, M. A., 1956a, Theory of propagation of elastic waves in a fluid-saturated porous solid. I. Low-frequency range: Journal of the Acoustical Society of America, **28**, 168–178, doi: [10.1121/1.1908239](https://doi.org/10.1121/1.1908239).
- Biot, M. A., 1956b, Theory of propagation of elastic waves in a fluid-saturated porous solid. II. Higher-frequency range: Journal of the Acoustical Society of America, **28**, 179–1191, doi: [10.1121/1.1908241](https://doi.org/10.1121/1.1908241).
- Biot, M. A., 1962a, Mechanics of deformation and acoustic propagation in porous media: Journal of Applied Physics, **33**, 1482–1498, doi: [10.1063/1.1728759](https://doi.org/10.1063/1.1728759).
- Biot, M. A., 1962b, Generalized theory of acoustic propagation in porous dissipative media: Journal of the Acoustical Society of America, **34**, 1254–1264, doi: [10.1121/1.1918315](https://doi.org/10.1121/1.1918315).
- Bracewell, R. N., 1978, The Fourier transform and its applications: McGraw-Hill Book Company.
- Burridge, R., and J. B. Keller, 1981, Poroelasticity equations derived from microstructure: Journal of the Acoustical Society of America, **70**, 1140–1146, doi: [10.1121/1.386945](https://doi.org/10.1121/1.386945).
- Calvert, R., 2005, Insights and methods for 4D reservoir monitoring and characterization: EAGE/SEG Distinguished Instructor Short Course 8.
- Chapman, C. H., 2004, Fundamentals of seismic wave propagation: Cambridge University Press.
- Chen, J., J. W. Hopmans, and M. E. Grismer, 1999, Parameter estimation of two-fluid capillary pressure — Saturation and permeability functions: Advances in Water Resources, **22**, no. 5, 479–493, doi: [10.1016/S0309-1708\(98\)00025-6](https://doi.org/10.1016/S0309-1708(98)00025-6).
- Courant, R., and D. Hilbert, 1962, Methods of mathematical physics: Wiley Interscience.
- Dean, R., X. Gai, C. Stone, and S. Minkoff, 2006, A comparison of techniques for coupling porous flow and geomechanics: Society of Petroleum Engineers Journal, **11**, no. 1, 132–140, doi: [10.2118/79709-PA](https://doi.org/10.2118/79709-PA).
- de la Cruz, V., and T. J. T. Spanos, 1985, Seismic wave propagation in a porous medium: Geophysics, **50**, 1556–1565, doi: [10.1190/1.1441846](https://doi.org/10.1190/1.1441846).
- de Marsily, G., 1986, Quantitative hydrogeology: Academic Press.
- Domenico, S. N., 1974, Effects of water saturation on seismic reflectivity of sand reservoirs encased in shale: Geophysics, **39**, 759–769, doi: [10.1190/1.1440464](https://doi.org/10.1190/1.1440464).
- Domenico, S. N., 1976, Effect of brine-gas mixture on velocity in an unconsolidated sand reservoir: Geophysics, **41**, 882–894, doi: [10.1190/1.1440670](https://doi.org/10.1190/1.1440670).
- Dvorkin, J., R. Nolen-Hoeksema, and A. Nur, 1994, The squirt-flow mechanism: Macroscopic description: Geophysics, **59**, 428–438, doi: [10.1190/1.1443605](https://doi.org/10.1190/1.1443605).
- Dvorkin, J., and A. Nur, 1998, Acoustic signatures of patchy saturation: International Journal of Solids and Structures, **35**, 4803–4810, doi: [10.1016/S0020-7683\(98\)00095-X](https://doi.org/10.1016/S0020-7683(98)00095-X).
- Frenkel, J., 1944, On the theory of seismic and seismoelectric phenomena in a moist soil: Journal of Physics (in Russian), **8**, 230–241.
- Friedlander, F. G., and J. B. Keller, 1955, Asymptotic expansions of solutions of $(\nabla^2 + k^2)u = 0$: Communications on Pure and Applied Mathematics, **8**, no. 3, 387–394, doi: [10.1002/cpa.3160080306](https://doi.org/10.1002/cpa.3160080306).
- Gajo, A., and L. Mongiovi, 1995, An analytical solution for the transient response of saturated linear elastic porous media: International Journal of Numerical and Analytical Methods in Geomechanics, **19**, no. 6, 399–413, doi: [10.1002/nag.1610190603](https://doi.org/10.1002/nag.1610190603).
- Garg, S. K., 1971, Wave propagation effects in a fluid-saturated porous solid: Journal of Geophysical Research, **76**, 7947–7962, doi: [10.1029/JB076i032p07947](https://doi.org/10.1029/JB076i032p07947).
- Garg, S. K., and A. H. Nayfeh, 1986, Compressional wave propagation in liquid and/or gas saturated elastic porous media: Journal of Applied Physics, **60**, 3045–3055, doi: [10.1063/1.337760](https://doi.org/10.1063/1.337760).
- Johnson, D. L., 2001, Theory of frequency dependent acoustics in patchy-saturated porous media: Journal of the Acoustical Society of America, **110**, 682–694, doi: [10.1121/1.1381021](https://doi.org/10.1121/1.1381021).
- Johnson, D. L., J. Koplik, and R. Dashen, 1987, Theory of dynamic permeability and tortuosity in fluid-saturated porous media: Journal of Fluid Mechanics, **176**, no. 1, 379–402, doi: [10.1017/S0022112087000727](https://doi.org/10.1017/S0022112087000727).
- Kline, M., and I. W. Kay, 1979, Electromagnetic theory and geometrical optics: John Wiley and Sons.
- Korsunsky, S., 1997, Nonlinear waves in dispersive and dissipative systems with coupled fields: Addison Wesley Longman.
- Kosten, C. W., and C. Zwikker, 1941, Extended theory of the absorption of sound by compressible wall-coverings: Physica, **8**, no. 9, 968–978, doi: [10.1016/S0031-8914\(41\)80004-4](https://doi.org/10.1016/S0031-8914(41)80004-4).
- Kravtsov, Y. A., and Y. I. Orlov, 1990, Geometrical optics of inhomogeneous media: Springer-Verlag.
- Levy, T., 1979, Propagation of waves in a fluid-saturated porous elastic solid: International Journal of Engineering Science, **17**, no. 9, 1005–1014, doi: [10.1016/0020-7225\(79\)90022-3](https://doi.org/10.1016/0020-7225(79)90022-3).
- Lo, W.-C., G. Sposito, and E. Majer, 2002, Immiscible two-phase fluid flows in deformable porous media: Advances in Water Resources, **25**, no. 8–12, 1105–1117, doi: [10.1016/S0309-1708\(02\)00050-7](https://doi.org/10.1016/S0309-1708(02)00050-7).
- Lo, W.-C., G. Sposito, and E. Majer, 2005, Wave propagation through elastic porous media containing two immiscible fluids: Water Resources Research, **41**, W02025, doi: [10.1029/2004WR003162](https://doi.org/10.1029/2004WR003162).
- Luneburg, R. K., 1966, Mathematical theory of optics: University of California Press.
- Masson, Y. J., S. R. Pride, and K. T. Nihei, 2006, Finite difference modeling of Biot's poroelastic equations at seismic frequencies: Journal of Geophysical Research, **111**, B10305, doi: [10.1029/2006JB004366](https://doi.org/10.1029/2006JB004366).
- Minkoff, S. E., C. Stone, S. Bryant, and M. Peszynska, 2004, Coupled geomechanics and flow simulation for time-lapse seismic modeling: Geophysics, **69**, 200–211, doi: [10.1190/1.1649388](https://doi.org/10.1190/1.1649388).
- Minkoff, S. E., C. Stone, S. Bryant, M. Peszynska, and M. Wheeler, 2003, Coupled fluid flow and geomechanical deformation modeling: Journal of Petroleum Science and Engineering, **38**, no. 1–2, 37–56, doi: [10.1016/S0920-4105\(03\)00021-4](https://doi.org/10.1016/S0920-4105(03)00021-4).
- Mualem, Y., 1976, A new model for predicting the hydraulic conductivity of unsaturated porous media: Water Resources Research, **12**, 513–522, doi: [10.1029/WR012i003p00513](https://doi.org/10.1029/WR012i003p00513).
- Murphy, W. F., 1982, Effects of partial water saturation on attenuation in Massillon sandstone and Vycor porous glass: Journal of the Acoustical Society of America, **71**, 1458–1468, doi: [10.1121/1.387843](https://doi.org/10.1121/1.387843).
- Noble, B., and J. W. Daniel, 1977, Applied linear algebra: Prentice-Hall.
- Noorshad, J., C.-F. Tsang, and P. A. Witherspoon, 1992, Theoretical and field studies of coupled behaviour of fractured rocks — I. Development and verification of a numerical simulator: International Journal of Rock Mechanics and Mining Sciences & Geomechanics Abstracts, **29**, no. 4, 401–409, doi: [10.1016/0148-9062\(92\)90515-2](https://doi.org/10.1016/0148-9062(92)90515-2).
- Press, W. H., S. A. Teukolsky, W. T. Vetterling, and B. P. Flannery, 1992, Numerical recipes: Cambridge University Press.
- Pride, S. R., 2005, Relationships between seismic and hydrological properties, in S. R. Pride, ed., Hydrogeophysics: Springer, 253–291.
- Pride, S. R., A. F. Gangi, and F. D. Morgan, 1992, Deriving the equations of media for isotropic motion: Journal of the Acoustical Society of America, **92**, 3278–3290, doi: [10.1121/1.404178](https://doi.org/10.1121/1.404178).
- Pride, S. R., F. D. Morgan, and A. F. Gangi, 1993, Drag forces of porous-medium acoustics: Physical Review B, **47**, no. 9, 4964–4978, doi: [10.1103/PhysRevB.47.4964](https://doi.org/10.1103/PhysRevB.47.4964).

- Rubin, Y., and S. S. Hubbard, 2006, *Hydrogeophysics*: Springer.
- Rutqvist, J., Y. S. Wu, C. F. Tsang, and G. Bodvarsson, 2002, A modeling approach for analysis of coupled multiphase fluid flow, heat transfer, and deformation in fractured porous rock: *International Journal of Rock Mechanics and Mining Sciences & Geomechanics Abstracts*, **39**, no. 4, 429–442, doi: [10.1016/S1365-1609\(02\)00022-9](https://doi.org/10.1016/S1365-1609(02)00022-9).
- Santos, J. E., J. M. Corbero, and J. Douglas Jr., 1990, Static and dynamic behavior of a porous solid saturated by a two-phase fluid: *Journal of the Acoustical Society of America*, **87**, 1428–1438, doi: [10.1121/1.399439](https://doi.org/10.1121/1.399439).
- Sethian, J. A., 1985, Curvature and the evolution of fronts: *Communications in Mathematical Physics*, **101**, no. 4, 487–499, doi: [10.1007/BF01210742](https://doi.org/10.1007/BF01210742).
- Sethian, J. A., 1999, *Level set and fast marching methods*: Cambridge University Press.
- Silvester, J. R., 2000, Determinants of block matrices: *The Mathematical Gazette*, **84**, 460–467.
- Simon, B. R., O. C. Zienkiewicz, and D. K. Paul, 1984, An analytical solution for the transient response of saturated porous elastic solids: *International Journal for Numerical and Analytic Methods in Geomechanics*, **8**, no. 4, 381–398, doi: [10.1002/nag.1610080406](https://doi.org/10.1002/nag.1610080406).
- Slattery, J. C., 1968, Multiphase viscoelastic fluids through porous media: *American Institute of Chemical Engineering Journal*, **14**, no. 1, 50–56, doi: [10.1002/aic.690140112](https://doi.org/10.1002/aic.690140112).
- Slattery, J. C., 1981, *Momentum, energy, and mass transfer in continua*: Robert E. Krieger Publishing.
- Stahl, S., 1997, *Introductory modern algebra*: John Wiley & Sons.
- Tuncay, K., 1995, Wave propagation in single- and double-porosity deformable porous media saturated by multiphase fluids: Ph.D. thesis, Texas A&M University.
- Tuncay, K., and M. Y. Corapcioglu, 1996, Body waves in poroelastic media saturated by two immiscible fluids: *Journal of Geophysical Research*, **101**, no. B11, 25149–25159, doi: [10.1029/96JB02297](https://doi.org/10.1029/96JB02297).
- Tuncay, K., and M. Y. Corapcioglu, 1997, Wave propagation in poroelastic media saturated by two fluids: *Journal of Applied Mechanics*, **64**, no. 2, 313–320, doi: [10.1115/1.2787309](https://doi.org/10.1115/1.2787309).
- van Genuchten, M. T., 1980, A closed-form equation for predicting the hydraulic conductivity of unsaturated soils: *Soil Science Society of America Journal*, **44**, no. 5, 892–898, doi: [10.2136/sssaj1980.03615995004400050002x](https://doi.org/10.2136/sssaj1980.03615995004400050002x).
- Vasco, D. W., 2008, Modeling quasi-static poroelastic propagation using an asymptotic approach: *Geophysical Journal International*, **173**, 1119–1135, doi: [10.1111/gji.2008.173.issue-3](https://doi.org/10.1111/gji.2008.173.issue-3).
- Vasco, D. W., 2009, Modelling broad-band poroelastic propagation using an asymptotic approach: *Geophysical Journal International*, **179**, 299–318, doi: [10.1111/gji.2009.179.issue-1](https://doi.org/10.1111/gji.2009.179.issue-1).
- Vasco, D. W., 2011, On the propagation of a coupled saturation and pressure front: *Water Resources Research*, **47**, W03526, doi: [10.1029/2010WR009740](https://doi.org/10.1029/2010WR009740).
- Vasco, D. W., and S. E. Minkoff, 2009, Modelling flow in a pressure-sensitive, heterogeneous medium: *Geophysical Journal International*, **179**, 972–989, doi: [10.1111/gji.2009.179.issue-2](https://doi.org/10.1111/gji.2009.179.issue-2).
- Vidale, J., 1988, Finite-difference calculation of travel times: *Bulletin of the Seismological Society of America*, **78**, 2062–2076.
- Wang, R., and H.-J. Kumpel, 2003, Poroelasticity: Efficient modeling of strongly coupled, slow deformation processes in a multilayered half-space: *Geophysics*, **68**, 705–717, doi: [10.1190/1.1567241](https://doi.org/10.1190/1.1567241).
- Whitham, G. B., 1974, *Linear and nonlinear waves*: John Wiley and Sons.
- Wyckoff, R. D., and H. G. Botset, 1936, The flow of gas-liquid mixtures through unconsolidated sands: *Physics*, **7**, no. 9, 325–345, doi: [10.1063/1.1745402](https://doi.org/10.1063/1.1745402).